RSC Advances

REVIEW

View Article Online
View Journal | View Issue

Cite this: *RSC Adv.*, 2023, **13**, 19429

Recent advances in fluorescent materials for mercury(II) ion detection

Qiuping Li *[a] and You Zhou *[b]

Invading mercury would cause many serious health hazards such as kidney damage, genetic freak, and nerve injury to human body. Thus, developing highly efficient and convenient mercury detection methods is of great significance for environmental governance and protection of public health. Motivated by this problem, various testing technologies for detecting trace mercury in the environment, food, medicines or daily chemicals have been developed. Among them, the fluorescence sensing technology is a sensitive and efficient detection method for detecting Hg^{2+} ions due to its simple operation, rapid response and economic value. This review aims to discuss the recent advances in fluorescent materials for Hg^{2+} ion detection. We reviewed the Hg^{2+} sensing materials and divided them into seven categories according to the sensing mechanism: static quenching, photoinduced electron transfer, intramolecular charge transfer, aggregation-induced emission, metallophilic interaction, mercury-induced reactions and ligand-to-metal energy transfer. The challenges and prospects of fluorescent Hg^{2+} ion probes are briefly presented. We hope that this review can provide some new insights and guidance for the design and development of novel fluorescent Hg^{2+} ion probes to promote their applications.

Received 11th April 2023
Accepted 14th June 2023

DOI: 10.1039/d3ra02410e

rsc.li/rsc-advances

1. Introduction

With the development of industries, the risk of exposure to various harmful heavy metal ions also increases.[1–4] In particular, environmental pollution caused by mercury and its compounds has always attracted great attention because they could invade the human body *via* breathing, skin contact or food chain, and enrich in the human body.[5–9] According to the HSAB (hard and soft acids and bases) theory, the mercury ion (Hg^{2+}) is a typical soft acid that can strongly react with molecules or materials rich in atoms such as O, N, and S.[10–12] Once the Hg^{2+} ion enters the human body, it can easily bind with groups such as carboxyl, amino, and phosphate, especially those molecules bearing sulphydryl (–SH) or disulfide (–S–S–) groups. Then, it affects the work of many proteins, enzymes or genes and causes various diseases such as kidney damage[13–15]

[a]*Key Laboratory of Chronic Diseases, School of Pharmacy, Fuzhou Medical College of Nanchang University, Fuzhou 344000, China*
[b]*State Key Laboratory Base of Novel Functional Materials and Preparation Science, School of Materials Science and Chemical Engineering, Ningbo University, Ningbo 315211, China*

Qiuping Li received BS from Lanzhou University and earned a PhD in Inorganic Chemistry from Tongji University in Shanghai. After graduation, he joined Ningbo University of Technology and worked there until 2021. Currently, he works in the Fuzhou Medical College of Nanchang University. His research interests are in the field of fluorescent materials, focusing on the build-up of lanthanide-based hybrid materials with sensing or lighting applications.

You Zhou received his PhD degree in 2016 from the Department of Chemistry, Tongji University. Now he is an associated professor in the School of Materials Science and Chemical Engineering Ningbo University. His current interests involve chemo-/bio-sensors and photoluminescent functional materials.

and gene tampering.[16–18] Thus, developing a cheap and fast Hg^{2+} detecting method is of great significance for environmental governance and public health protection.[19–22]

Many effective methods such as atomic absorption spectrometry (AAS), atomic emission spectrometry (AES), inductively coupled plasma-atomic emission spectrometry (ICP-AES), electrochemical analysis, colorimetric method, and fluorescence analysis method have been developed for detecting Hg^{2+}. Among them, the fluorescence analysis method[23–26] has been widely used for detecting Hg^{2+} ions. It has advantages such as high sensitivity and selectivity, fast response, low cost and suitability for *in vivo* detection. Given the huge advantage of fluorescent materials, many fluorescent materials based on gold nanoparticles,[27] metal–organic framework materials,[28] carbon materials,[29] polymer-based materials or rhodamine family compounds[30] have been developed for Hg^{2+} ion sensing.

Considering the variety of luminescent sensing materials used for Hg^{2+} ion detection, this review will mainly focus on the recent advances in Hg^{2+} sensing materials based on different sensing implementation schemes. We made a systematic exposition to the design ideas and sensing mechanisms of existing Hg^{2+} ion sensing materials. Meanwhile, the problems and challenges in this field are also discussed. Moreover, we hope that this review would be helpful to the researchers working on Hg^{2+} sensors or the other people engaged in sensing material development.

2. Classification of mercury ion fluorescent probes

By 2022, hundreds of luminescent sensors that can be used for detecting Hg^{2+} ions were reported. These Hg^{2+} ion probes can be mainly classified according to their sensing mechanisms as follows:

(1) Fluorescent sensors based on the static quenching mechanism. This type of sensor usually has fluorescence, but once it coordinates with Hg^{2+} ions, the fluorescence intensity of the resulting product would decrease significantly, leading to an obvious "turn-off" fluorescence phenomenon.

(2) Fluorescent sensors involved in the photoinduced electron transfer (PET) process. Some materials usually have weak fluorescence due to the PET effect, but once they react with Hg^{2+} ions, the original PET process is suppressed, resulting in a fluorescence enhancement phenomenon. In another case, the sensor did not have PET effect at the beginning, and it emitted intense fluorescence. After the introduction of Hg^{2+} ions, a PET process will appear to suppress the fluorescence of the sensor.

(3) Fluorescent sensors involved in the influence of intramolecular charge transfer (ICT) process. This type of sensor contains both electron withdrawing and donating groups, which would cause charge separation under the excitation of light. Its fluorescence properties are greatly affected by the ICT state. When the sensor interacts with Hg^{2+} ions, the ICT process will be affected, resulting in the redistribution of electron density on the sensor, which will cause changes in fluorescence intensity or spectrum shape.

(4) Fluorescent sensors involved in aggregation-induced emission (AIE). Compounds with AIE property usually show weak or no fluorescence emission at lower concentrations. Introducing Hg^{2+} ions can cause the aggregation of compounds, which would restrict the intramolecular motion of them, resulting in significantly enhanced fluorescence emission.

(5) Fluorescent sensors involved in the metallophilic interaction. These sensors are mainly composed of noble metal nanoclusters (especially gold nanoclusters), which usually display "turn-off" fluorescence upon reacting with Hg^{2+} ions.

(6) Fluorescent sensors based on the mercury-induced reaction. Such sensors are not simply bound to Hg^{2+} ions, but when it binds to Hg^{2+} ions, it would cause obvious structural transformation, resulting in a change in fluorescence.

(7) Fluorescent sensors based on the changes in ligand-to-metal energy transfer (LMET). This kind of sensor is usually represented by lanthanide-based fluorescent materials. When Hg^{2+} ions interact with certain groups of the sensor, the LMET process is affected, leading to a decrease or increase in the fluorescence emission of lanthanide ions.

Of course, still there are some Hg^{2+} sensors which cannot be simply classified into categories depending on their design principle. In addition, the above-mentioned classification is not absolute, and many fluorescent sensors often involve multiple sensing mechanisms.[31–35] To help readers better understand the recent development of Hg^{2+} ion sensors, in this review, we will divide and classify the sensors according to their main sensing mechanism (Fig. 1).

3. Fluorescent sensor based on the static quenching mechanism

Static quenching is one of the most common fluorescence sensing mechanisms. Generally, sensor materials have fluorescence. When they combine with a quencher, a fluorescent inert complex will form, causing a "turn-off" fluorescence quenching change.[36–38] Hg^{2+} ions have good coordination ability to the groups containing N, O, and S atoms, and most of the resulting complexes are fluorescent inert. Therefore, researchers can design fluorescence sensing materials for Hg^{2+} detection based on this mechanism. It is noteworthy that static quenching will not affect the fluorescence lifetime (τ) of the sensor. Meanwhile, such quenching can also be recovered upon the addition of some reagents with strong binding preference to Hg^{2+} ions, *e.g.*, sulfide or chelating agents.[39–41] Therefore, researchers could easily decide whether the quenching mechanism is a static quenching process based on these two characteristics. Besides, the Stern–Volmer equation is usually used to determine if it is static quenching or dynamic quenching, or both.[42–44]

Masuhara *et al.*[45] earlier reported the examples of closed-shell heavy metal ion sensing based on non-fluorescent complex formation and proposed a fluorescence static quenching mechanism. Saleh[46] has also recommended that this static quenching mechanism could be used to explain the sensing reaction involving the formation of ground-state non-fluorescent complexes. Based on their research, compounds

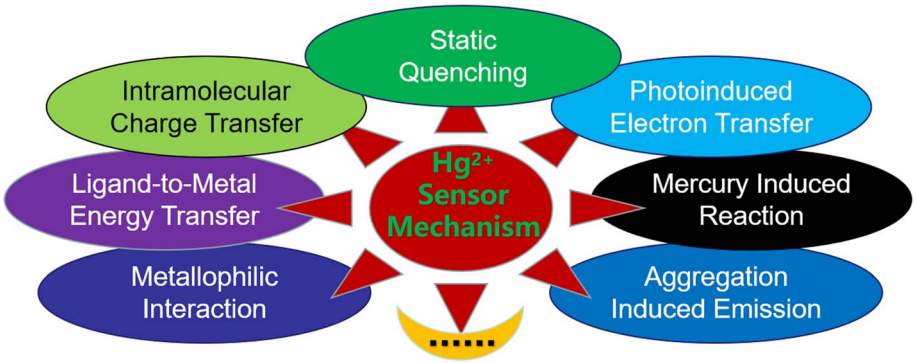

Fig. 1 Sensing mechanisms of Hg^{2+} ion probes classified based on their main mechanism.

with sulphur-containing receptors, macrocycles or aromatic units could usually be used to detect Hg^{2+} ions by fluorescence static quenching mechanism involving intersystem crossing. Various compounds with a crown ether structure showed sensitive fluorescence turn-off properties targeting Hg^{2+} ions.[47–49] Manna *et al.*[50] prepared a porous covalent organic framework nanosheet (abbreviated as Mc-CONs) by linking the rigid diamine building block comprising cyclic naptho-1,4-dithia-15-crown-5 units through a β-ketoenamine linker (Fig. 2). It was found that napthodithia-crown-ether moieties on Mc-CONs can serve as an efficient catcher for Hg^{2+} ions, making the electron transfer from the extended π-conjugated network of Mc-CONs to the empty orbital of Hg^{2+} ions. Therefore, the resulting Mc-CON has the ability to detect and effectively remove ultra-trace levels of Hg^{2+} ions from aqueous solution simultaneously. Besides, Mc-CONs are robust materials, and their Hg^{2+} ion removal efficiency would remain almost unaffected after several cycles of regeneration over a wide range of pH 3–9, which makes them promising materials for the remediation of Hg^{2+} ion pollution.

Since fluorescent carbon dots (CDs) have advantages such as low toxicity, good biological compatibility, good water solubility, and high photo-stability, their application value in heavy metal detection has naturally received widespread attention.[51–54] Functionalized CDs, especially those with surfaces rich in carboxyl, sulfhydryl, amino groups and so on, are easily combined with heavy metals differently, usually resulting in non-fluorescent complexes, and the fluorescence quenching mechanism is mainly involved in static quenching. Wu *et al.*[55] had synthesized nitrogen-doped carbon quantum dots (N-CQDs) by a microwave hydrothermal method using citric acid and urea as sources (Fig. 3). The resulting N-CQDs emitted blue fluorescence, had a high fluorescence quantum yield up to 62.67%, and showed good selectivity and low detection limits to Hg^{2+} ion detection. The sensing behavior revealed a static quenching mechanism according to the measurement of the fluorescence lifetime methods. Meanwhile, due to the good water solubility, the N-CQD was also made into a kind of fluorescent invisible ink. Because N-CQDs have good biocompatibility and low cytotoxicity, they are successfully used for imaging and the detection of Hg^{2+} ions in HeLa cells.

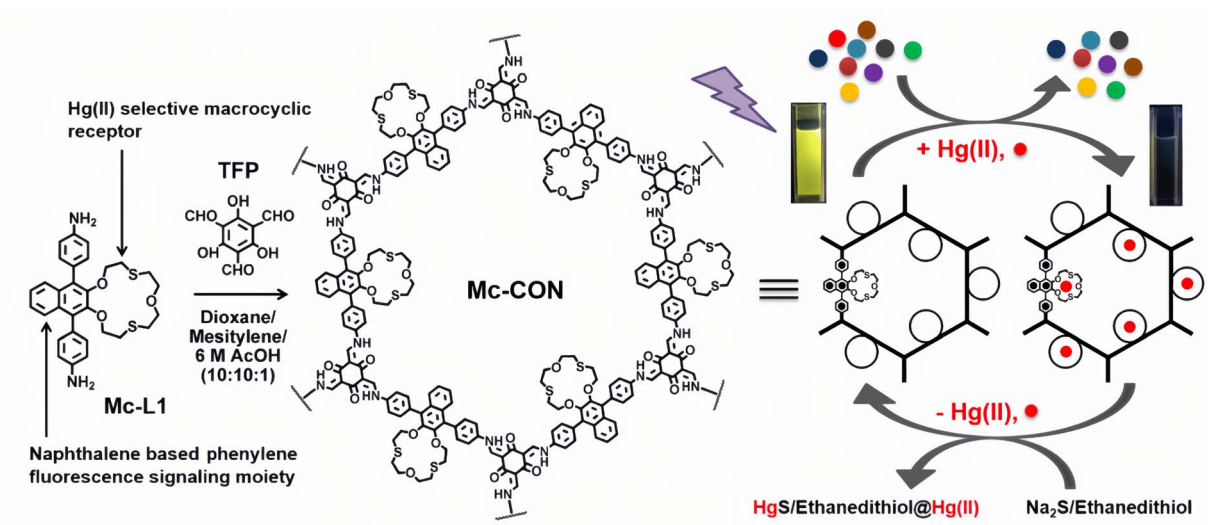

Fig. 2 Scheme of the preparation of Mc-CON and its application in sensing and removing Hg^{2+} ions in water. Reproduced with permission from ref. 50. Copyright 2021, American Chemical Society.

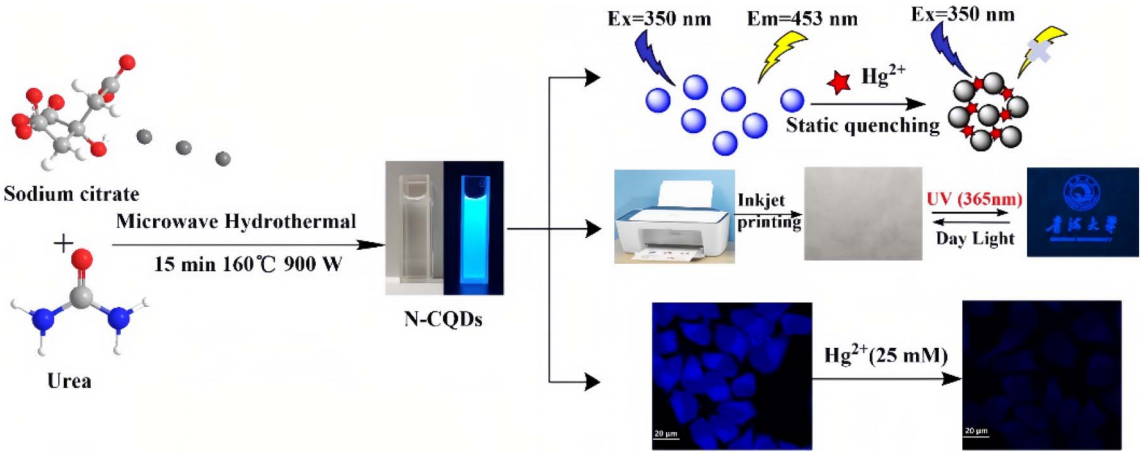

Fig. 3 Schematic illustration of the synthetic route and applications of N-CQDs. Reproduced with permission from ref. 55. Copyright 2022, John Wiley and Sons.

Rapidly developed fluorescent MOFs have also been widely used in the detection of various metal ions in the past few years.[56–59] Ghosh *et al.*[60] had designed and synthesized a Zr-based UiO-66 MOF (denoted as IITG-5a) using a benzo[1,2-*b*:4,5-*b*]dithiophene-2,6-dicarboxylic acid linker. The soft sulphur (S) atoms of the thiophene rings in the linker molecule can interact with the soft Hg^{2+} ions effectively, thus provide the MOF an outstanding selectivity sensing property towards the Hg^{2+} ions (Fig. 4). The response time of IITG-5a in the cases of sensing Hg^{2+} ions was 1 min, and the corresponding limit of detection (LOD) values were as low as 5 nm. The fluorescence lifetime analysis revealed no significant change before (2.08 ns) and after (2.07 ns) addition of Hg^{2+} ions, indicating that the fluorescence changes followed the static quenching mechanism. IITG-5a was further used to produce test strips that showed a real-time monitoring ability to Hg^{2+} ions. Besides, they found that the IITG-5a could be used to detect nitrofurazone or nitrofurantoin in MeOH.

R. V. Rathod *et al.*[61] prepared a novel fluorescein-phenylalaninol (FPA) conjugate by an environmentally benign mechanochemistry-assisted method. They found that the FPA molecule can serve as a colorimetric and fluorescent sensor for the simultaneous detection and removal of Hg^{2+} ions in aqueous solutions *via* the formation of the complex with Hg^{2+} ions (Fig. 5). Based on the Stern–Volmer equation, the fluorescence process follows a static quenching mechanism. The LOD of FPA for Hg^{2+} ions is 0.34 μM as determined by fluorescence spectroscopic methods. The FPA can also be used to develop a portable test strip, which can provide a rapid and straightforward detection of Hg^{2+} ions in all three states. Of course, many other kinds of materials could be designed and fabricated for sensing Hg^{2+} ions based on this mechanism.[62–64]

4. Fluorescent sensors involved in the PET process

A photoinduced electron transfer system usually consists of three parts, namely, a fluorophore, a connecting arm and an object acceptor. Typically, the acceptor is an electron donor whose HOMO is in a higher energy orbital than the energy of the HOMO of fluorophore. When the electron in the HOMO of fluorophore gets excited and leaves a vacancy, an electron from the HOMO of acceptor will transfer to this lower energy orbital, inhibiting the excited electron in the LUMO of fluorophore to return to the HOMO of fluorophore, thereby effectively quenching the fluorescence. If the acceptor binds to Hg^{2+} ions, the energy of HOMO of acceptor would be lowered, whereafter the excited electron in the LUMO of fluorophore can transition

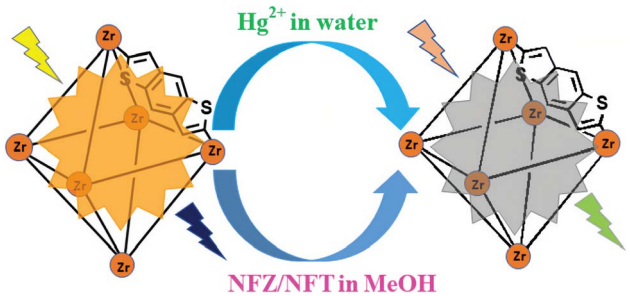

Fig. 4 Fluorogenic switch-off sensing of Hg^{2+} and NFT/NFZ by IITG-5a. Reproduced with permission from ref. 60. Copyright 2014, Royal Society of Chemistry.

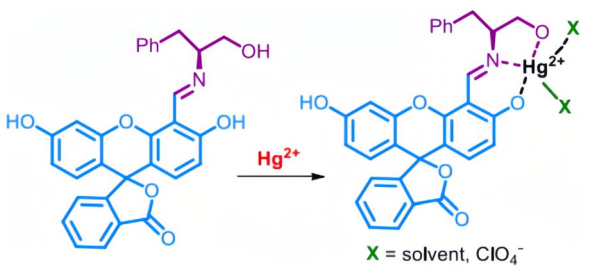

Fig. 5 Proposed binding of Hg^{2+} ions to FPA. Reproduced with permission from ref. 61, copyright 2020, American Chemical Society.

back to the HOMO of fluorophore, accompanying the emission of fluorescence. That is, the electron transfer in the above-mentioned process will be inhibited, leading to a "turn-on" fluorescence behavior, realizing the sensor detection of Hg^{2+} ions.

Extensive research has demonstrated that this "turn-on"-type fluorescence caused by the restriction of the PET process of sensors is a very effective means of detecting Hg^{2+} ions.[65–67] For example, Nolan *et al.*[68] designed a molecular sensor with a low fluorescence quantum yield due to the PET effect of the lone pair on the nitrogen atom of the aniline moiety. Coordination with Hg^{2+} will destroy the quenching pathway, resulting in an emission maximum red shift and a quantum yield increase, making it a useful Hg^{2+} ion sensor. Recently, Srivastava *et al.*[69] have designed and synthesized a novel hydrophilic PET sensor of Hg^{2+} ions (Fig. 6). The sensor has an anthracene core as a fluorophore along with two benzhydryl moieties and piperazine units as a suitable object acceptor because the benzhydryl and anthracene moieties connected by piperazine (the connecting arm) will form a stable hydrophilic PET system. Meanwhile, the soft closed-shell cation Hg^{2+} has a pronounced affinity to the acceptor and promotes a stable complex in an aqueous medium, which will restrict the PET process and lead to a real-time fluorescence "turn-on" response. The probe showed high selectivity and sensitivity for Hg^{2+} ions. As Hg^{2+} ions are gradually added to the sensor solution, a naked-eye-sensitive fluorescent color change (blue to blue-green) can be observed. Based on such switched-on fluorescence property, they had successfully used the sensor to detect Hg^{2+} ions in real contaminated water samples and live cell imaging.

In contrast, the new reverse PET process in materials often causes "urn-off" fluorescence, which has also been shown to be useful in designing Hg^{2+} ion sensors.[70–72] Hou *et al.*[73] synthesized a novel zinc phosphonate with a one-dimensional chain structure based on (2,4,6-trimethylbenzene-1,3,5-triyl) tris(methylene)triphosphonic acid (H_4L) and 2,2′-biimidazole (2,2′-biim). The as-synthesized [Zn(H_4L)(2,2′-biim)] can act as a highly selective fluorescent probe for Hg^{2+} ions. According to the investigation of DFT calculations, the HOMO energy of 2,2′-biim (acceptor) increased from −5.440 eV to −5.030 eV after it chelated with Hg^{2+} ions, and was higher than the HOMO energy of H_6L–Zn (−5.133 eV, fluorophore) (Fig. 7). Hence, the electron in the HOMO of 2,2′-biim would transfer into the vacancy in HOMO of H_6L–Zn left by the excited electron, preventing the return of excited electrons in the LUMO to HOMO of H_6L–Zn. Thereby, [Zn(H_4L)(2,2′-biim)] exhibited a fluorescence quenching property *via* the PET mechanism, which gave it the ability to detect Hg^{2+} ions. In addition, they also prepared a [Zn(H_4L)(2,2′-biim)] test strip, which had been used to quickly detect Hg^{2+} ions with naked eyes under UV irradiation.

5. Fluorescent sensors involved in the ICT process

Many fluorophores contain both an electron-donating group (donor) and an electron-withdrawing group (acceptor). Under the excitation of light, the electron in the donor can transfer to the acceptor (ICT), following the increase in charge separation within the fluorophore. Such fluorophore usually has a large Stokes shift and solvatochromic effect. Because the Hg^{2+} ion has strong affinity with electrons, it can easily combine with the donor moiety of the fluorophore and affect the ICT. Meanwhile, the fluorescence properties of the fluorophore are greatly affected by the ICT state.

Molecules with ICT processes and the ability to coordinate with Hg^{2+} ions are usually involved in the above-mentioned mechanism, making them useful Hg^{2+} ion sensors.[74–80] For

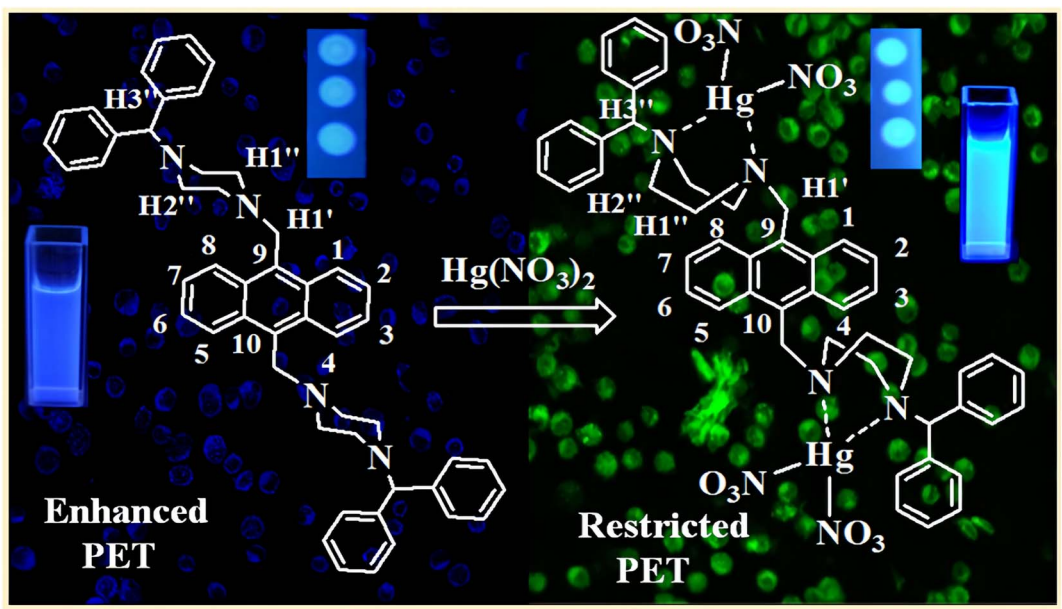

Fig. 6 Proposed binding of Hg^{2+} ions to the sensor. Reproduced with permission from ref. 69, copyright 2014, American Chemical Society.

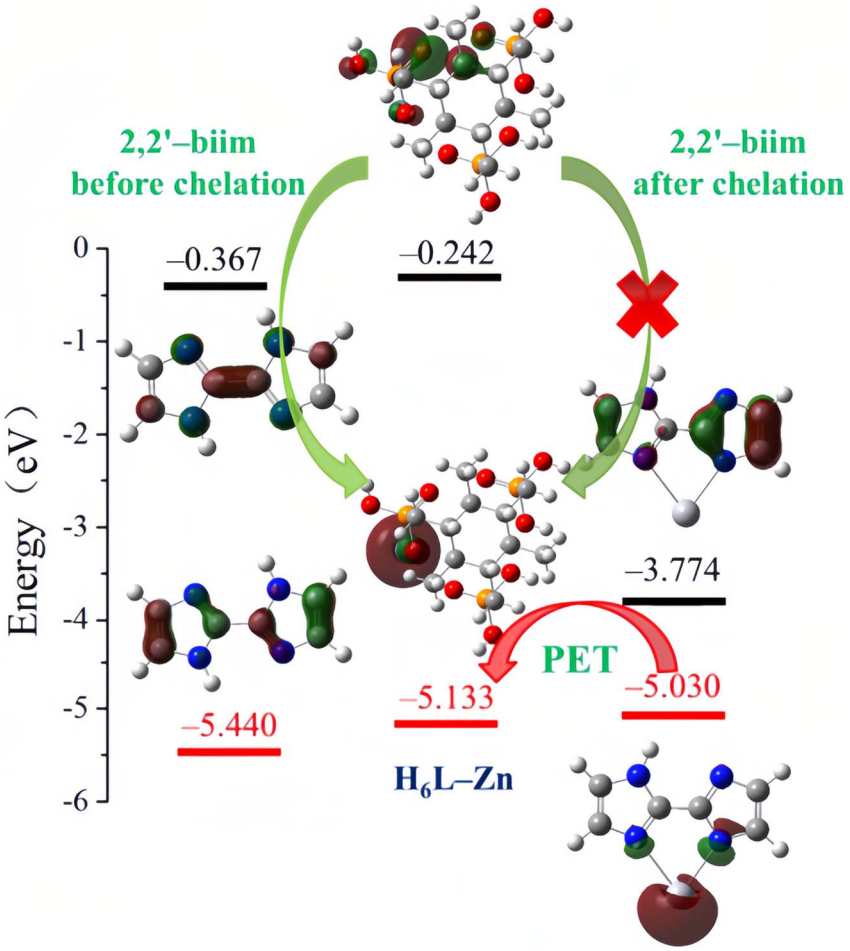

Fig. 7 LUMO and HOMO energies calculated for 2,2-biim, H_6L–Zn and Hg–2,2-biim. Reproduced with permission from ref. 73, copyright 2020, Elsevier.

example, Wang *et al.*[81] synthesized a fluorophore with a strong "push–pull" π-electron system, under light excitation, the fluorophore will undergo an ICT from the donor to the acceptor, and the resulting fluorescence has a long emission wavelength due to the large extent of π-electron conjugation. However, when the coordination part (which is also the electron donor) contacts a Hg^{2+} ion, its electron donor capacity will be decreased, resulting in the blue shift of absorption and emission spectra due to the decrease in π-electron conjugation. Thus, the molecule can be used as a fluorescent sensor for detecting Hg^{2+} ions. Recently, Wei *et al.*[82] have developed a novel fluorescent probe DGRK based on the tripeptide (Gly–Arg–Lys–NH_2) conjugated with a dansyl fluorophore (Fig. 8). The peptide-based DGRK exhibited excellent water solubility and showed bright yellow fluorescence under 365 nm UV light. However, when Hg^{2+} combine with the DGRK molecule, the ICT process between the amino group of the tripeptide structure (donor) and the dansyl group (acceptor) would be changed, and the resulting DGRK–Hg^{2+} complex only has very weak fluorescence emission. They found that the fluorescence of DGRK solutions can be quenched only with the addition of Hg^{2+} ions, and the response time is very rapid (40 s) and the sensitivity is very high (LOD = 33.6 nM). Furthermore, they had further extended the resulting DGRK–Hg^{2+} complex to develop a S^{2-} sensor based on the strong binding affinity of Hg^{2+} to S^{2-}. Additionally, due to the low toxicity and good bio-compatibility of DGRK, the authors had successfully used it to monitor Hg^{2+} and S^{2-} in living cells, and developed smartphone-based test strips, which had high sensitivity, stability and selectivity for Hg^{2+} ion detection.

Meng *et al.*[83] had designed and synthesized a novel molecule composed of a conjugated fluorophore structure (2,1,3-benzothiadiazole = BTD) and an acceptor moiety (rhodamine-3-acetic = RDA) (Fig. 9 top). According to DFT calculations, the electron density of HOMO and LUMO for BTD–RDA is mainly localized on 2,1,3-benzothiadiazole, the benzene ring and the rhodanine part, which clearly suppressed the ICT process, resulting in a weak fluorescence emission. After binding with Hg^{2+} ions, the electron density of the HOMO for BTD–RDA–Hg^{2+} localized on the acetic acid site will shift to 2,1,3-benzothiadiazole, the benzene ring and the rhodanine moiety during transition to LUMO. The calculation results show that the energy difference of the HOMO–LUMO level for the probe BTD–RDA (2.849 eV) reduces significantly when it binds to Hg^{2+} ions. The energy difference of the HOMO–LUMO level for the resulting BTD–RDA–Hg^{2+} complex is calculated as 0.899 eV, which make it

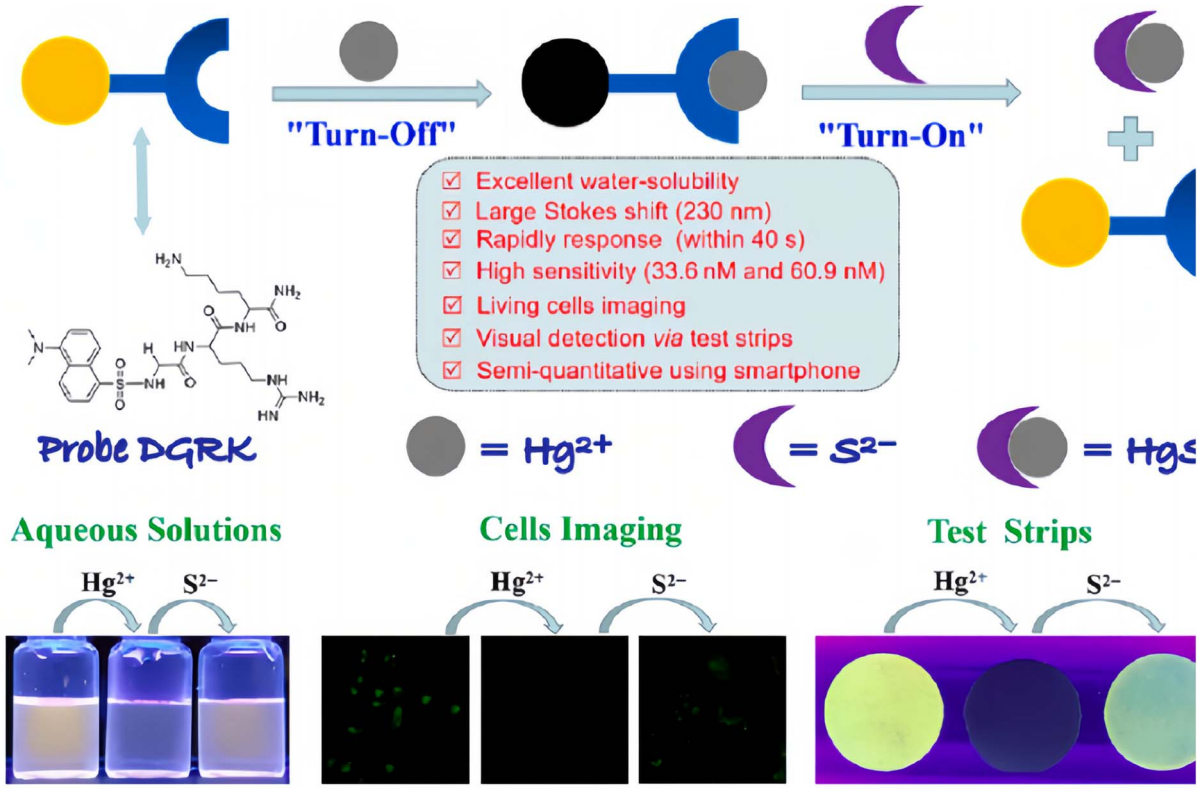

Fig. 8 Schematic diagram of the molecular structure and sensing mechanism of probe DGRK, and its application highlights. Reproduced with permission from ref. 82, copyright 2023, Elsevier.

energetically favorable for the ICT process (Fig. 9). Thus, once BTD–RDA binds with Hg^{2+} ions, an efficient ICT process between RDA and BTD is realized, leading to a fluorescence "turn-on" phenomenon that makes BTD–RDA a possible Hg^{2+} ion detection sensor. It has been proven that BTD–RDA can be used as a visual indicator of the presence of Hg^{2+} ions under UV and be used to detect Hg^{2+} ions in living cells and zebrafish.

6. Fluorescent sensors involved in the AIE process

The research of AIE compounds stems from the work of Tang and co-workers.[84–88] Compounds with AIE properties usually have free intramolecular rotation or vibration (or both) in dilute solutions, which would consume their excited-state energy, resulting in weak or no luminescence. When these AIE compounds are induced to aggregate by certain substances, the intramolecular rotation or vibration is suppressed, and therefore, the resulting aggregate emits intense fluorescence. Besides, the AIE active molecules have a high quantum yield, a large Stokes shift and good stability, all of which have made them attract increasing attention over the past decades. AIE phosphors have become important fluorescent probes due to their "turn-on" property when targeting certain compounds. Naturally, they have been widely used in detecting Hg^{2+} ions over the past dozen years.[89–101]

Some molecules with thymine units can coordinate with Hg^{2+} ions, resulting in the AIE phenomenon.[102–104] Zhang *et al.*[105] synthesized a novel AIE phosphor with a triphenylamine–triazine motif and a thymine unit. The resulting compound showed very weak emission before the addition of Hg^{2+} ions. Upon addition of Hg^{2+} ions, the compounds aggregated into nanoparticles due to the coordination of thymine moieties with Hg^{2+} ions (Fig. 10). It had been proven that the compound is a sensitive and selective fluorescent "turn-on" sensor for Hg^{2+} ions. In addition, the nano-aggregation also remarkably enhanced the two-photon fluorescence of the compound. Under the excitation of an 800 nm laser, the nano-aggregator emitted intense red fluorescence, making it highly desirable for biological imaging applications.

Yang *et al.*[106] had synthesized a multiple-response fluorescent compound by the condensation reaction of 5-bromosalicylaldehyde and 2-benzothiazoleacetonitrile. The resulting compound is an "AIE transformer" that exhibits different aggregated states in different solutions and thus emits different light. Different aggregated states give the compound the ability to detect H_2S and Hg^{2+} respectively. As shown in Fig. 11, Hg^{2+} ions can bind with the S atom and destroy the hydrogen bond (S···H–N), inducing the aggregated state change from AIE (3) to AIE (4) along with markedly different fluorescence emissions. Besides, they had demonstrated that such AIE transformers can be used for the selective detection of H_2S and Hg^{2+} in cells.

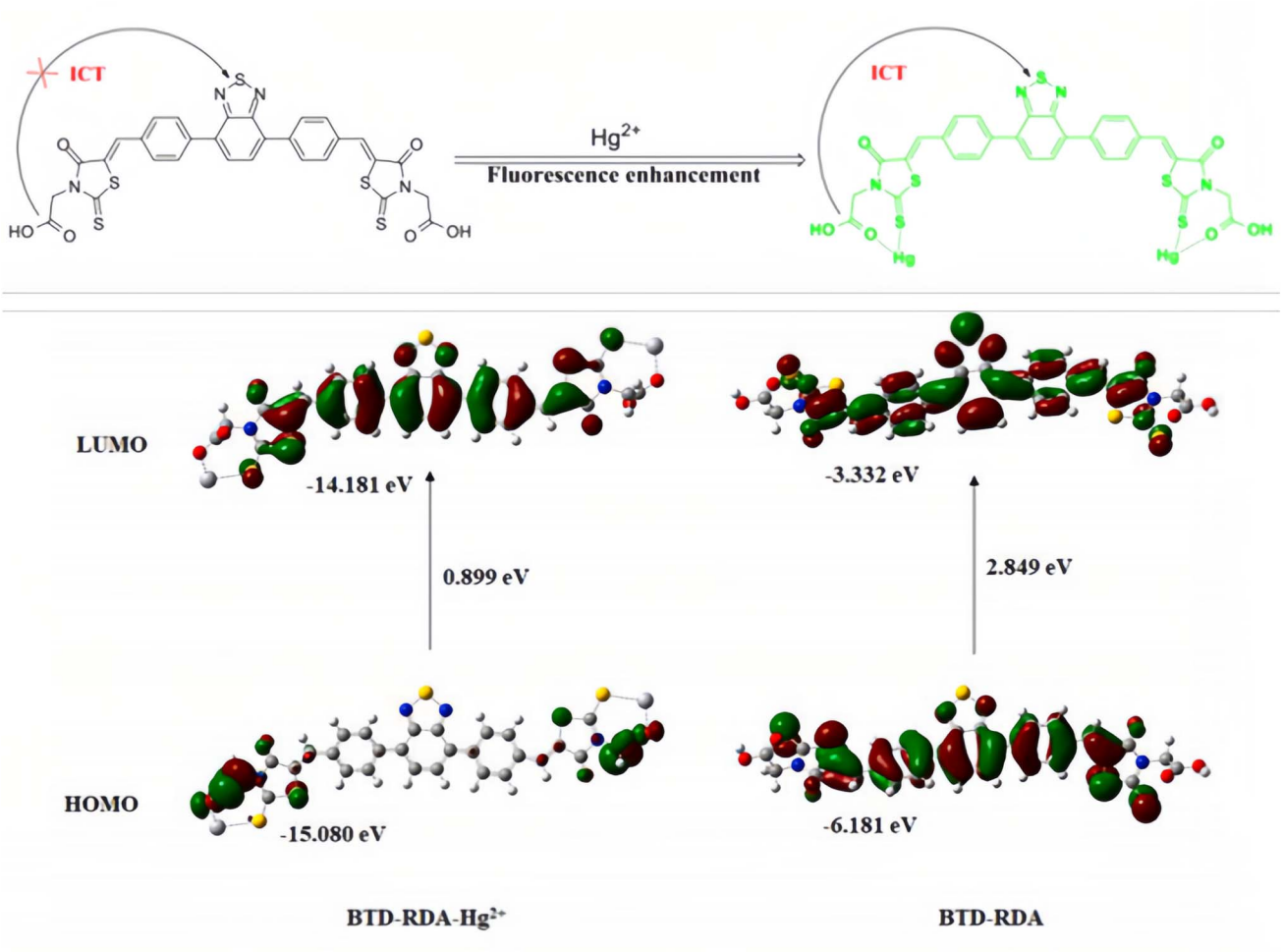

Fig. 9 Molecular structure of probe BTD–RDA (top); HOMO–LUMO energy diagrams of BTD–RDA with Hg^{2+} ions. Reproduced with permission from ref. 83, copyright 2021, Elsevier.

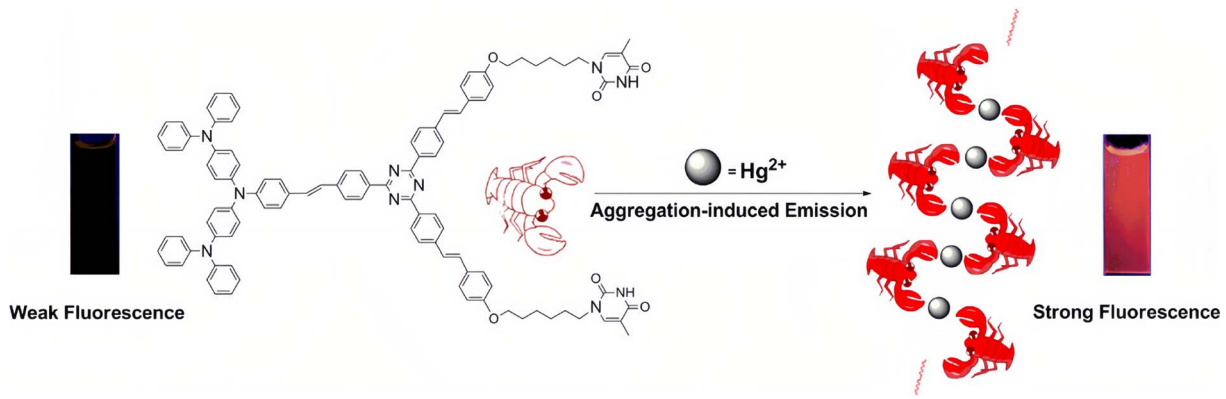

Fig. 10 Schematic illustration of the coordination mode between the probe and Hg^{2+}. Reproduced with permission from ref. 105, copyright 2013, Elsevier.

Besides, Liu *et al.*[107] had reported another mechanism for Hg^{2+} ion detection based on AIE phosphors. They prepared a novel dehydroabietic acid derivative with a quinoxaline moiety (denoted as DBAQ). DBAQ can well dissolve in a pure MeCN solution with a quite weak fluorescence emission while water was a poor solvent for it. When water is gradually added to the DBAQ solution (in MeCN), the fluorescence emission of the mixture was almost the same as the one of pure DBAQ solution (in MeCN). Nevertheless, once the content of water reaches 80% or above, an unexpectedly strong fluorescence emission was observed. This was mainly due to the aggregation of DBAQ when water was added as a poor solvent, which results in an AIE

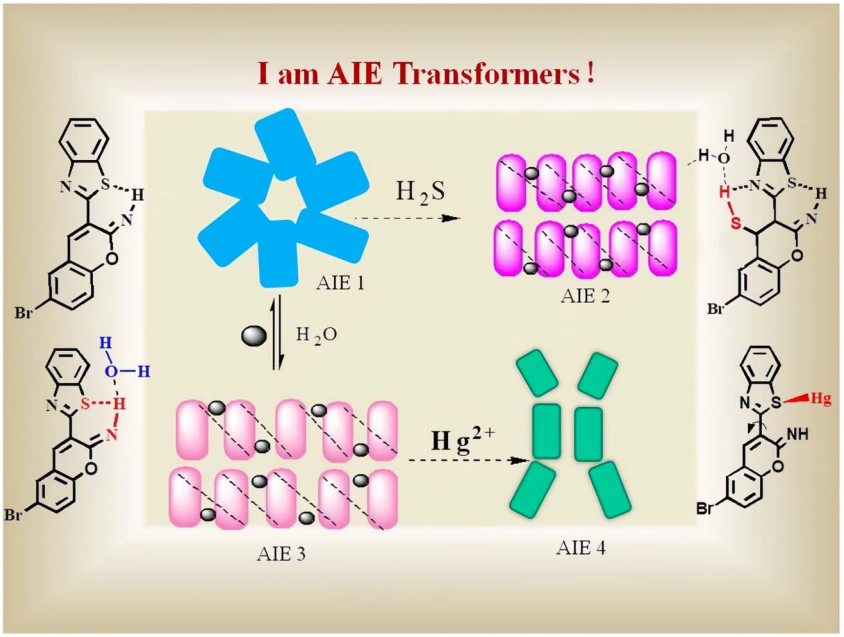

Fig. 11 Schematic illustration of the probe with H_2S and Hg^{2+} in different aggregation states. Reproduced with permission from ref. 106, copyright 2019, Elsevier.

phenomenon. They had found that the fluorescence intensity of the DBAQ solution in the MeCN/H_2O solution (v/v = 1/9, pH = 7.5) at 600 nm dropped off sharply upon addition of excess Hg^{2+} ions. Meanwhile, the fluorescence of the DBAQ solution changed from bright orange to colorless under a 365 nm UV lamp. They found that after adding Hg^{2+} ions, the mean diameter of the DBAQ aggregator became larger instead of becoming smaller, which ruled out that the fluorescence quenching was not caused by the change of DBAQ with no longer aggregation or dissolution due to the introduction of Hg^{2+} ions. The probable fluorescence quenching mechanism of DBAQ towards Hg^{2+} ions (Fig. 12): (i) the combination of the nitrogen atom with Hg^{2+} ions interrupted the intramolecular conjugation and (ii) the resulting DBAQ–Hg^{2+} complex has a strong spin–orbit coupling effect, causing the "turn-off" fluorescence phenomenon. Finally, they had demonstrated that DBAQ can be used as an effectively probe for detecting Hg^{2+} ions in environmental water, seafood samples and living organisms. Many other reports[108–110] have also observed a similar phenomenon, during which static quenching may occur because the AIE phosphor and Hg^{2+} ions would form a fluorescent inert complex. And it seems that this fluorescence "turn-off" strategy of the AIE phosphor has a great potential application for designing effective Hg^{2+} ion probes.

7. Fluorescent sensors involved in metallophilic interactions

Metal nanoclusters (MNCs) composed of a small number of atoms such as gold nanoclusters (AuNCs) and silver nanoclusters (AgNCs) usually show bright fluorescence because of

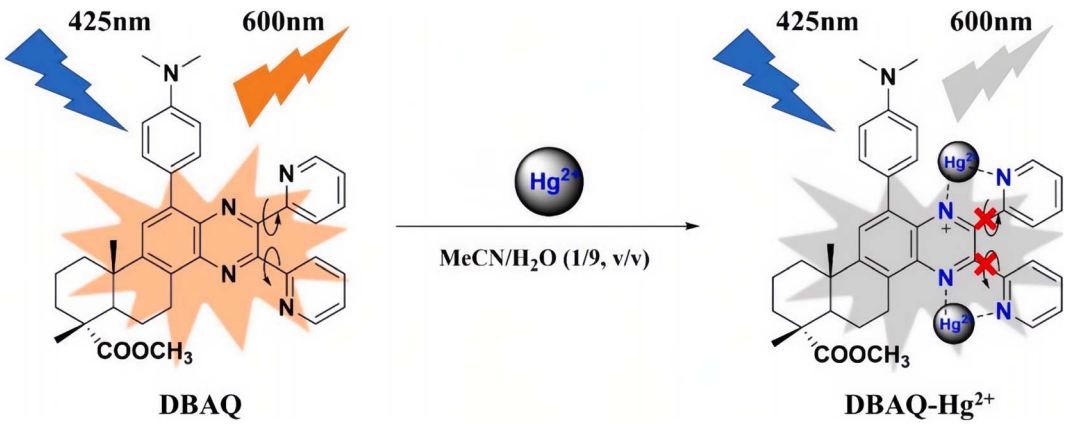

Fig. 12 Proposed sensing mechanism of DBAQ towards Hg^{2+}. Reproduced with permission from ref. 107, copyright 2022, Elsevier.

their unique discrete energy levels.[111] MCNs also have the advantages of water solubility, ultra-small size, good photostability, bio-compatibility and so on, which make them promising materials for sensing or imaging applications. Among them, AuNCs have become sensitive and selective fluorescent probes for the detection of Hg^{2+} ions based on the active $5d^{10}$–$5d^{10}$ metallophilic interaction between Hg^{2+} and Au^{+}.[112–120]

Initially, Lee *et al.*[121] found that Hg^{2+} ions can induce the aggregation of DNA–Au nanoparticles by forming T–Hg^{2+}–T coordination complexes, resulting in the color change of a DNA–Au nanoparticle solution at a certain temperature, thus making the detection of Hg^{2+} ions possible. Xie *et al.*[122] later reported that the metallophilic interaction between Hg^{2+} and Au^{+} could lead to fluorescence quenching of Au nanoparticles and, on this basis, proposed a new labeling free technique for detecting Hg^{2+}. Recently, Sahu *et al.*[123] have synthesized a novel AuNC with a L-cysteine-assisted chitosan reduction "one pot" synthetic protocol. The as-synthesized AuNCs (L-cys/CS–AuNC) have strong fluorescence emission at 575 nm. They had demonstrated that the L-cys/CS–AuNC could act as a selective and sensitive fluorescent probe for the detection of Hg^{2+} ions. The LOD of the L-cys/CS–AuNC in water was 3 nM, which was lower than the EPA standard for drinking water. Meanwhile, as shown in Fig. 13, the fluorescence quenching mechanism of the L-cys/CS–AuNC in the presence of Hg^{2+} ions was assigned to the strong $5d^{10}$–$5d^{10}$ metallophilic interaction between Hg^{2+} and Au^{+}. Besides, the L-cys/CS–AuNC has been shown to be successfully used in real water samples such as pond water, river water and tap water to detect Hg^{2+} ions.

8. Fluorescent sensors based on the mercury-induced reaction

As previously mentioned, the Hg^{2+} ion has a high affinity to electrons, which make them suitable for mercuration, desulfurization and coordination. The coordination of Hg^{2+} ions with O, N, S, *etc.*, may lead to a further reaction of the compound. Once the mercury-induced reactions could result in fluorescence changing, it could be used to design fluorescence sensing methods for detecting Hg^{2+} ions, which has been proven to be an effective sensing method.[124]

Hydroxy-mercury reaction is a typical electrophilic addition reaction that occurs between the unsaturated carbon bonds (double or triple bonds) and a mercury salt.[125–128] Based on this reaction, Tang *et al.*[129] had designed and synthesized a novel fluorescent probe, which can be used for the detection of Hg^{2+}

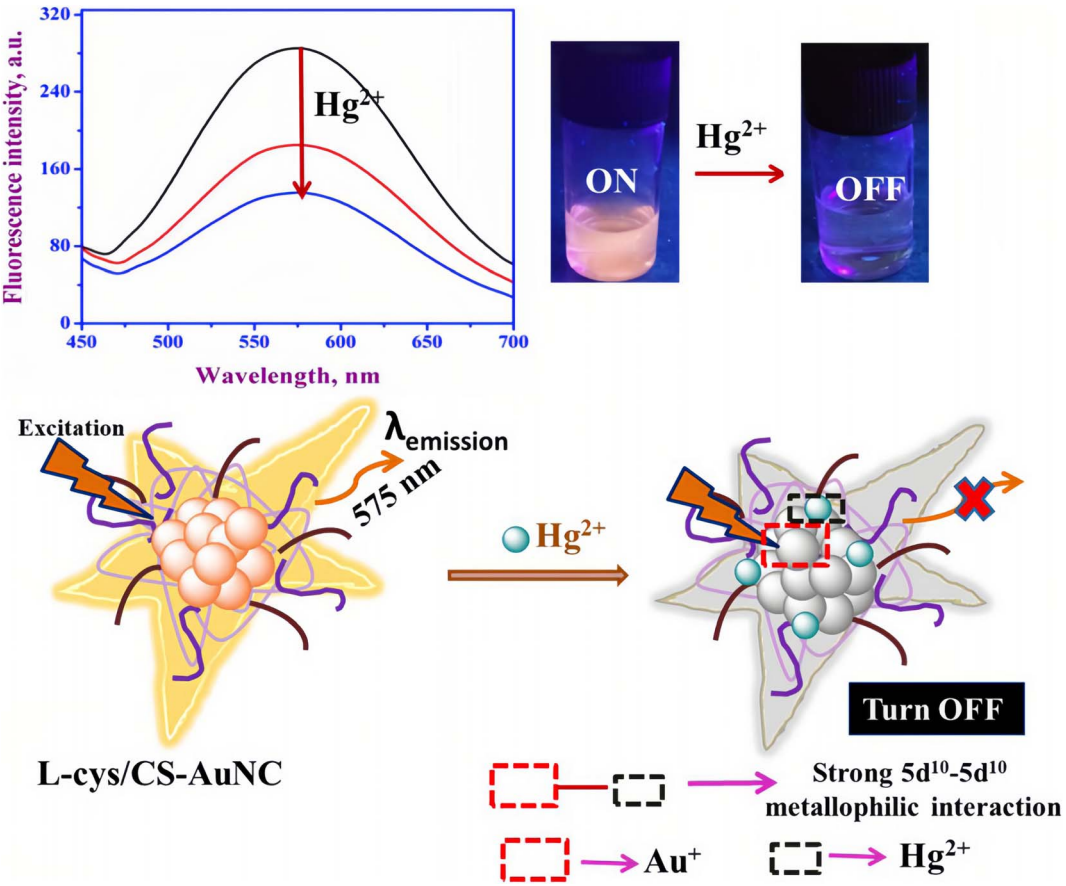

Fig. 13 Schematic of the sensing of Hg^{2+} ions by L-cys/CS–AuNC based on the Hg^{2+}–Au^{+} interaction. Reproduced with permission from ref. 123, copyright 2020, Elsevier.

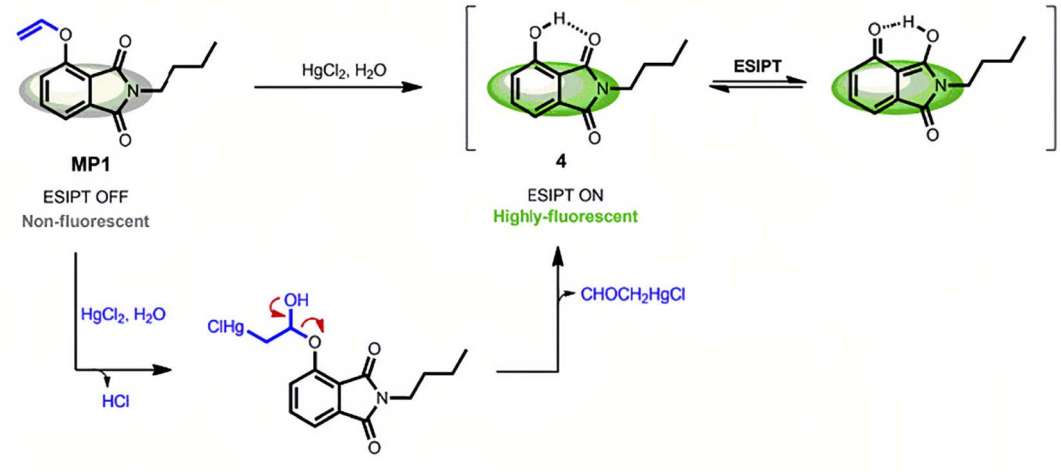

Fig. 14 Mercury-triggered hydrolysis of MP1. Reproduced with permission from ref. 129, copyright 2019, Elsevier.

ions. As shown in Fig. 14, the as-synthesized compound is a vinyl ether derivative of 3-hydroxyphthalimide (denoted as MP1). When targeting Hg^{2+} ions, vinyl ether of MP1 would undergo a Hg^{2+}-induced hydrolytic cleavage process, and then MP1 would turn into free ESIPT-active 3-hydroxyphthalimide, resulting in the recovery of green fluorescence emission by restoring the ESIPT process. This fluorescence "turn-on" property of MP1 had been demonstrated to be highly selective and sensitive in detecting Hg^{2+} ions in aqueous solutions with a low detection limit of 1.9 ppb. Besides, the MP1 had been successfully used to detect Hg^{2+} ions in live cells.

It is well known that the thymine base usually pairs with the adenine base in the DNA double helix. However, extensive research has found that a thymine will pair with another thymine *via* the meditation of Hg^{2+} ions to form a more stable thymine–Hg^{2+}–thymine (T–Hg^{2+}–T) pair. Since such reaction has high sensitivity and selectivity, it has also been used to develop the reaction-based fluorescent probe of Hg^{2+} ions.[130–134] For example, Li *et al.*[135] had designed a novel label-free fluorescence assay based on T-rich DNA, which can form a T–Hg^{2+}–T stable hairpin structure in the presence of Hg^{2+} ions. The resulting T–Hg^{2+}–T complex can facilitate fluorescence enhancement *via* intercalating with SYBR Green I (SG I), which acted as a fluorescent dye that had been widely used in analytic fields (Fig. 15). It had been proved to be a rapid, convenient and economic method for the detection of Hg^{2+} ions in environmental drinking water samples. Meanwhile, the method has high specificity for detecting Hg^{2+} ions, and its lowest detection limit can be as low as 3 nM.

Recently, reaction-based fluorescent probes by virtue of the strong thiophilic ability of Hg^{2+} ions have also attracted increasing attention.[136–139] Wang *et al.*[140] had constructed

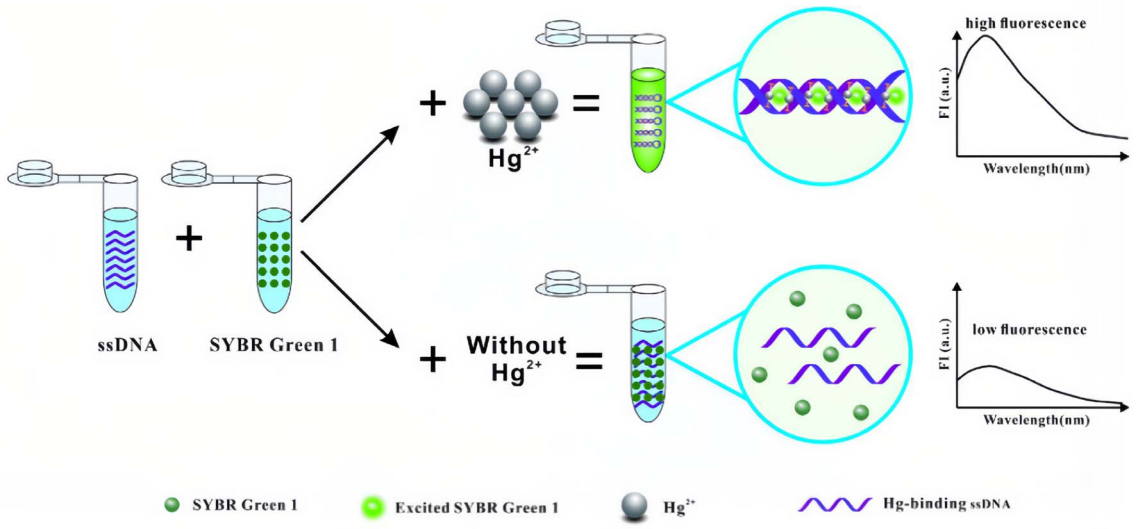

Fig. 15 Schematic illustration of the label-free fluorescence method for the detection of Hg^{2+}. Reproduced with permission from ref. 135, copyright 2017, Springer Nature.

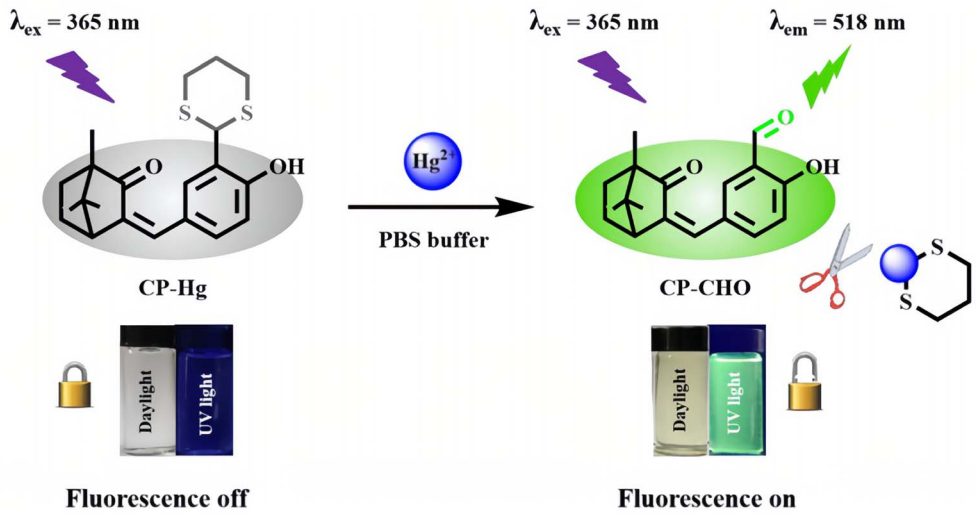

Fig. 16 Recognition mechanism of CP–Hg toward Hg^{2+}. Reproduced with permission from ref. 140, copyright 2020, American Chemical Society.

a fluorescent turn-on probe for Hg^{2+} ion recognition *via* a Hg^{2+} ion-induced thioacetal deprotection reaction. As shown in Fig. 16, the CP–Hg molecule employs camphor as a unique scaffold, and the 1,3-dithiane unit on it can be deprotected into a formyl group after the addition of Hg^{2+} ions, resulting in a fluorescence "turn-on" phenomenon. The resulting CP–Hg could act as a sensitive probe of Hg^{2+} ions with a detection limit of 19.3 nM. Meanwhile, CP–Hg-coated test strips were also successfully shown to be rapid and reliable tools for naked-eye detection of Hg^{2+} ions. In addition, CP–Hg could be used as a biomarker for fluorescence imaging of Hg^{2+} ions in living cells.

Rhodamine-based fluorescent chemosensors are another kind of reaction-based fluorescent probe of metal ions that has been widely studied. Early in 1997, Dujols *et al.*[141] reported a pioneering work using rhodamine-B hydrazide as a fluorescent chemodosimeter for Cu^{2+}. Since then, the application of rhodamine-B-derived compounds in the field of chemical sensing has gained great interest. There are many reviews on rhodamine-based chemosensors reported in the past decade.[142–144] Yang *et al.*[145] first used such rhodamine-based chemodosimeters for the rapid detection of Hg^{2+} ions in aqueous media, and achieved an amazing detection sensitivity below 2 ppb in aqueous solutions. The sensing mechanism of these probes is mainly based on the Hg^{2+} ion-induced structural conversion between the spirocyclic and open-cycle forms of rhodamine unit.[146–149] Recently, Vanjare *et al.*[150] have designed and synthesized a novel kind of rhodamine-based fluorescent probe of Hg^{2+} ions based on a rhodamine 6 G molecule. As shown in Fig. 17, the as-synthesized PS molecule is non-fluorescent, but a fluorescence "turn-on" behavior was observed when it targets Hg^{2+} ions due to the Hg^{2+} ion-induced ring-opening of the spiro-cyclic structure within a rhodamine moiety. The LOD for probe PS was determined to be 30.37 nM. Meanwhile, probe PS has been used to monitor Hg^{2+} ions in tap and drinking water with high selectivity to Hg^{2+} ions in the presence of additional metal ions. Besides, they had successfully used the probe PS in bio-imaging experiments for the

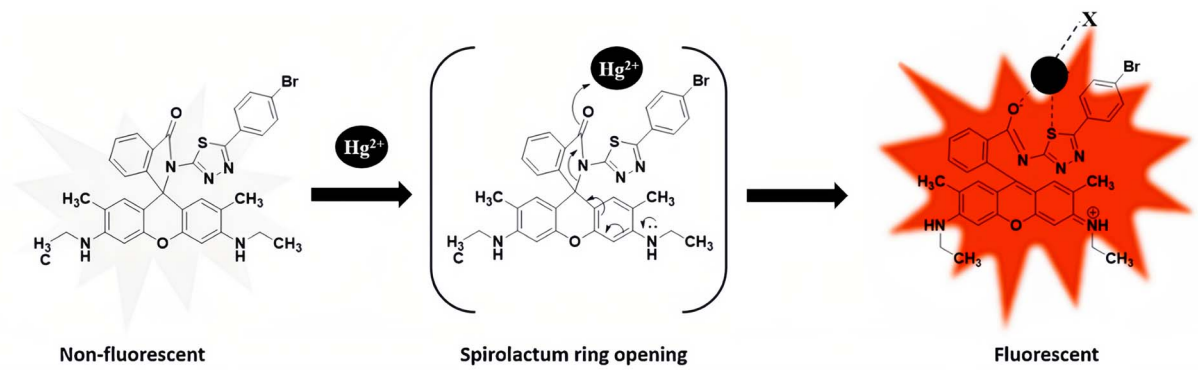

Fig. 17 Proposed binding mode of probe PS with Hg^{2+} metal ions (X = coordinating anion or solvent). Reproduced with permission from ref. 150, copyright 2021, Elsevier.

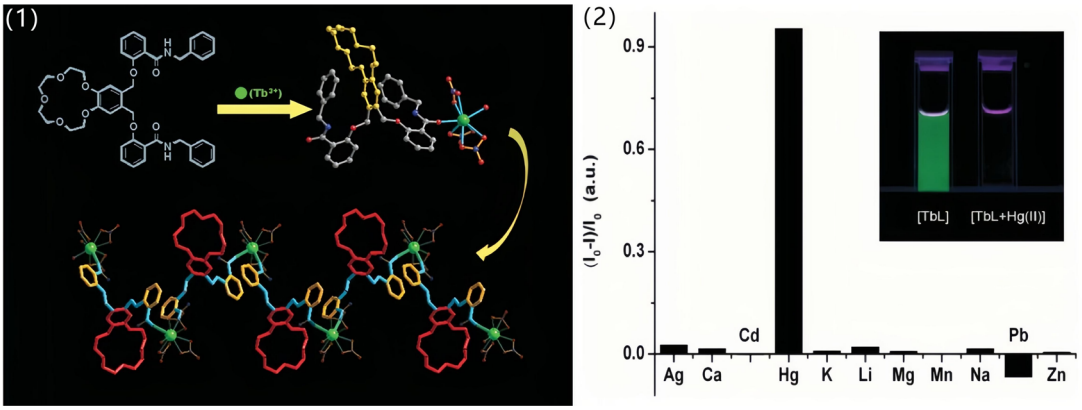

Fig. 18 (1) Structure of the ligand L, the asymmetric unit of the terbium complex and the structure view of the 1-D zig-zag coordination polymeric chain of the complex (left). (2) Quench ratio $[(I_0 - I)/I_0]$ of the luminescence intensity of the complex in methanol, with $[(n\text{-Bu})_4N]ClO_4$ as the supporting electrolyte, upon addition of 1.0 equiv. of different cations (excitation at 340 nm). Inset (upper right) shows the picture of the luminescence change of [TbL] upon addition of 0.50 equiv. of Hg^{2+} in methanol, illuminated by a standard laboratory UV lamp of 365 nm (right). Reproduced with permission from ref. 163, copyright 2010, Royal Society of Chemistry.

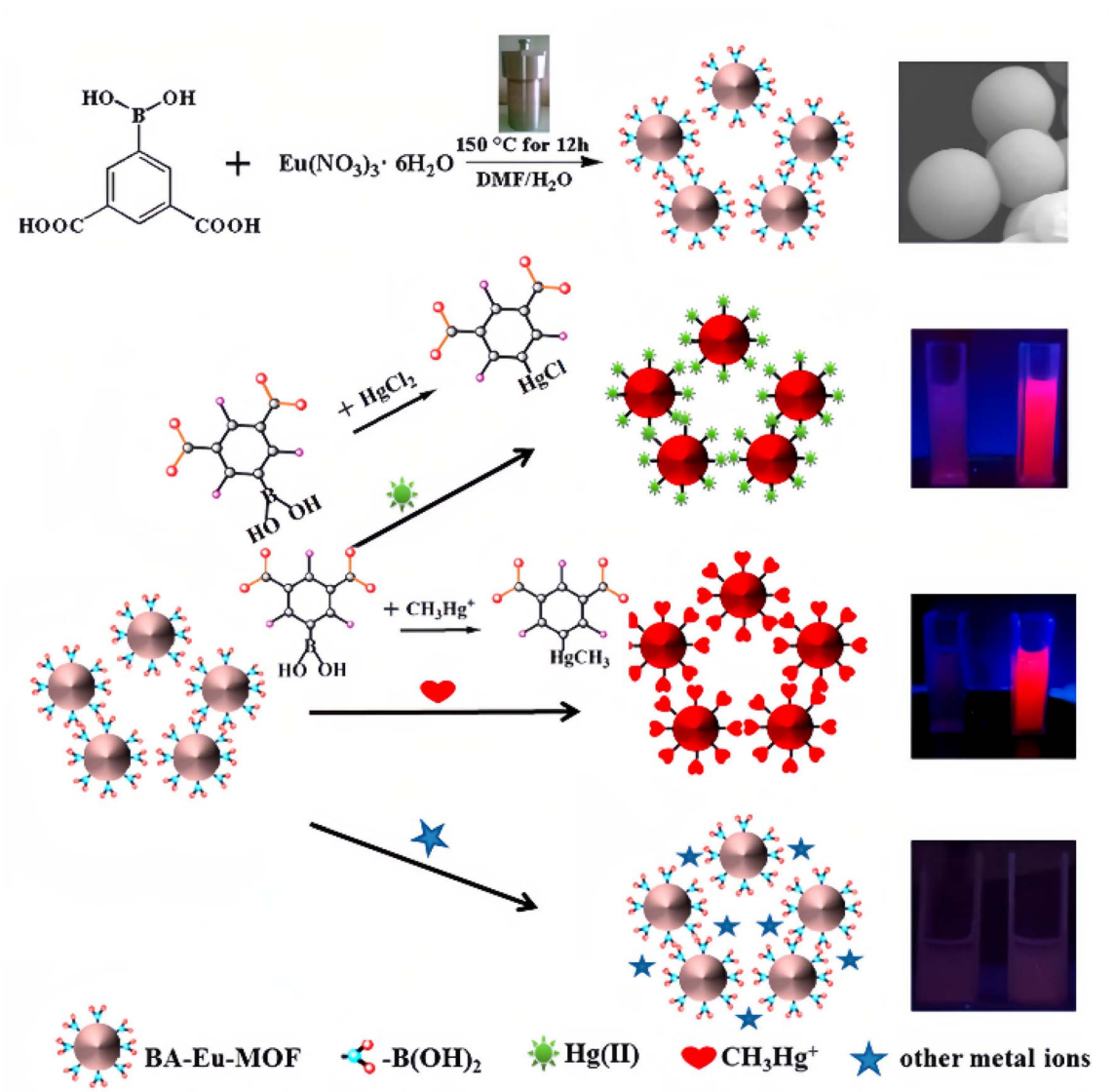

Fig. 19 BA–Eu-MOF synthesis and representation of the sensing process of BA–Eu-MOF toward Hg^{2+} and CH_3Hg^+ ions based on transmetalation. Reproduced with permission from ref. 169, copyright 2020, American Chemical Society.

detection of Hg^{2+} ions in MDA-MB-231 and A375 breast cancer cells.

Undoubtedly, owing to its high sensitivity and selectivity in detecting Hg^{2+} ions, reaction-based fluorescent probes have attracted increasing attention in the past few decades.

9. Fluorescent sensors involved in the LMET process

Lanthanide-based fluorescent materials exhibit linear emissions, long lifetimes and relatively independent emission spectra. Generally, lanthanide-based fluorescent probes are superior to others due to their strong resistance to background fluorescence interference. However, because the fluorescence of lanthanide materials mainly come from the f–f transition of lanthanide ions while the f → f transition is parity forbidden. Fortunately, this defect can be overcome by the introduction of an "antenna" unit that can effectively absorb the excitation energy, and then enhance the fluorescence intensity of lanthanide ions *via* a LMET process.[151–153] Interference to the LMET would inevitably lead to changes in the fluorescence of lanthanide-based materials. Based on this principle, many lanthanide-based fluorescent probes have been developed in recent years, including the sensor of Hg^{2+} ions.[154–162]

In 2010, Liu *et al.*[163] reported for the first time a highly selective Hg^{2+} ion probe based on the lanthanide complex. They designed and synthesized novel pendant benzo crown ether using a benzo-15-crown-5 unit as a macrocyclic receptor and *N*-benzylsalicylamide as a chromophore and coordination unit. As shown in Fig. 18 (left), the ligand L can chelate with Tb^{3+} ions by the oxygen atom of the amide group, while the macrocycle of the crown ether remains free. It has been proven that the as-synthesized terbium complex exhibits a strong green fluorescence due to the effective LMET from *N*-benzylsalicylamide to Tb^{3+} ions. Since the crown ether units still remain free and have a unique coordination capability with metal ions, the effects of various metal cations on the fluorescence properties of the terbium complex were investigated. As shown in Fig. 18 (right), the terbium complex showed immediate luminescence quenching only upon addition of Hg^{2+} ions, which make it a highly selective and sensitive fluorescent probe for detecting Hg^{2+} ions. It was inferred that the late reaction of the terbium complex with Hg^{2+} ions affected the LMET from *N*-benzylsalicylamide to Tb^{3+} ions, leading to fluorescence quenching.

The fluorescent probe based on lanthanide-functionalized MOFs has also attracted much attention as it can combine the characteristic photo-physical properties of lanthanide ions with the plentiful recognition site of MOFs.[164–168] Recently, Wang *et al.*[169] have developed a novel boric acid (BA)-functionalized lanthanide MOF (BA–Eu-MOF), which can be synthesized by a one-pot method with 5-boronobezene-1,3-dicarboxylic acid (5-bop) and Eu^{3+} ions (Fig. 19). Within the MOF, the 5-bop ligand acts as both the energy "antenna" of Eu^{3+} ions and the recognition units for Hg^{2+} and CH_3Hg^+ ions. Interestingly, the BA–Eu-MOF showed weak fluorescence in water because of the inefficient LMET caused by the electron-withdrawing effect of the BA group. But once the BA groups are replaced by Hg^{2+} or CH_3Hg^+ ions, the "antenna effect" would be greatly enhanced, re-activating the LMET from 5-bop to Eu^{3+} ions. Thus, an obvious fluorescence "turn-on" phenomenon would be observed when the BA–Eu-MOF encounters Hg^{2+} and CH_3Hg^+ ions. It has been proven that the BA–Eu-MOF can simultaneously detect Hg^{2+} and CH_3Hg^+ ions.

10. Summary and prospect

In summary, recent advances in fluorescent probes of Hg^{2+} ions related to the mechanism of static quenching, PET, ICT, AIE, metallophilic interaction, mercury-induced reaction and LMET were summarized and systematically discussed in this mini-review. In part two, we gave a brief introduction to each fluorescent probe from the perspective of sensing mechanism. Afterwards, the detailed sensing mechanism of each type of Hg^{2+} ion probe was discussed in each part, and the fluorescence characteristics of various sensors were also discussed. The response mechanism and implementation strategy of various probes for sensing Hg^{2+} ions were also presented and highlighted through selected examples. Among these probes, except for MNCs based on the metallophilic interaction mechanism, all other probes are due to the strong electron affinity of Hg^{2+} ions. The high electron affinity make Hg^{2+} ions easy to react with groups containing O, N, S atoms or unsaturated bonds, leading to coordination and even further reactions. It should be admitted that many reports on Hg^{2+} ion fluorescent probes are not included here, because they usually have unclear fluorescence sensing mechanism. Meanwhile, some Hg^{2+} ion fluorescent probes often have multiple sensing mechanisms. Thus, we classify the references according to their main sensor mechanism here.

As mentioned above, the sensing mechanism of Hg^{2+} ion fluorescent probes has developed to a certain extent, which can guide the design and synthesis of novel Hg^{2+} ion fluorescent probes. Although the research on Hg^{2+} ion fluorescent probes has made many impressive progresses, developing rapid Hg^{2+} ion fluorescent probes is still in the exploratory stage, and its practical applications face great challenges. For example, most reported probes focus on the detection of Hg^{2+} ions in water samples. However, Hg^{2+} ions in food, medicine, cosmetics or biological samples were less detected, and most need tedious preprocessing. Although most of the studies were focused on the detection, simultaneous removal of Hg^{2+} ions was rarely concerned. Besides, the sensing mechanism of some Hg^{2+} ion fluorescent probes was not clear, which hinders its further development and popularization. Therefore, to meet the increasing needs of mercury detection and pollution control, the following should be considered. First, the sensing mechanism of some Hg^{2+} ion fluorescent probes should be further explored, which will provide clear ideas for the design of novel probes. Second, the development of sensing methods based on green solvents (*e.g.* ionic liquid) can avoid polluting organic solvents, as well as using the unique solvent properties of ionic liquids to adapt more objects. Moreover, the probe with a solid support usually has good solution stability, and satisfactory

recyclability would be the hot spot in the future. In addition, it is urgent to develop more materials with dual functions of mercury detection and removal, which have great application prospects in environmental remediation.

Conflicts of interest

The authors declare that they have no known competing financial interests or personal relationships that could have appeared to influence the work reported in this paper.

Acknowledgements

This work was supported by the Science and Technology Research Project of Jiangxi Provincial Department of Education (GJJ218108), the National Natural Science Foundation of China (21701092), the Natural Science Foundation of Zhejiang Province (LY21B010002), the Natural Science Foundation of Ningbo (2021J105, 2022J104).

References

1 C. Zamora-Ledezma, D. Negrete-Bolagay, F. Figueroa, E. Zamora-Ledezma, M. Ni, F. Alexis and V. H. Guerrero, *Environ. Technol. Innov.*, 2021, **22**, 101504.
2 N. A. Qasem, R. H. Mohammed and D. U. Lawal, *npj Clean Water*, 2021, **4**, 1–15.
3 K. H. Vardhan, P. S. Kumar and R. C. Panda, *J. Mol. Liq.*, 2019, **290**, 111197.
4 J. P. Vareda, A. J. Valente and L. Durães, *J. Environ. Manage.*, 2019, **246**, 101–118.
5 O. Chastel, J. Fort, J. T. Ackerman, C. Albert, F. Angelier, N. Basu, P. Blévin, M. Brault-Favrou, J. O. Bustnes and P. Bustamante, *Sci. Total Environ.*, 2022, **844**, 156944.
6 K. Taux, T. Kraus and A. Kaifie, *Int. J. Environ. Res. Public Health*, 2022, **19**, 2081.
7 M. Shahid, S. Khalid, I. Bibi, J. Bundschuh, N. K. Niazi and C. Dumat, *Sci. Total Environ.*, 2020, **711**, 134749.
8 P. d. A. Rodrigues, R. G. Ferrari, L. N. Dos Santos and C. A. C. Junior, *J. Environ. Sci.*, 2019, **84**, 205–218.
9 M. C. Henriques, S. Loureiro, M. Fardilha and M. T. Herdeiro, *Reprod. Toxicol.*, 2019, **85**, 93–103.
10 S. Kamal, M. Khalid, M. S. Khan, M. Shahid and M. Ahmad, *Cryst. Growth Des.*, 2022, **22**, 3277–3294.
11 A. Pankajakshan, D. Kuznetsov and S. Mandal, *Inorg. Chem.*, 2019, **58**, 1377–1381.
12 Z. X. Wang and S. N. Ding, *Anal. Chem.*, 2014, **86**, 7436–7445.
13 E. Garcia-Pliego, M. Franco-Colin, P. Rojas-Franco, V. Blas-Valdivia, J. I. Serrano-Contreras, G. Pentón-Rol and E. Cano-Europa, *Food Funct.*, 2021, **12**, 2985–2994.
14 R. Abdeldayem, *Appl. Water Sci.*, 2022, **12**, 1–6.
15 B. Q. Han, Z. J. Lv, X. M. Han, S. Y. Li, B. Han, Q. Y. Yang, X. Q. Wang, P. F. Wu, J. Y. Li and N. Deng, *Biol. Trace Elem. Res.*, 2022, **200**, 1591–1597.
16 Q. L. Zhang, Z. X. Dong, Z. W. Luo, M. Zhang, X. Y. Deng, J. Guo, F. Wang and L. B. Lin, *J. Hazard. Mater.*, 2020, **389**, 121842.
17 L. X. Yang, Y. Y. Zhang, F. F. Wang, Z. D. Luo, S. J. Guo and U. Strähle, *Chemosphere*, 2020, **245**, 125586.
18 R. N. Monastero, C. Vacchi-Suzzi, C. Marsit, B. Demple and J. R. Meliker, *Toxics*, 2018, **6**, 35.
19 S. Ali, M. Mansha, N. Baig and S. A. Khan, *Chem. Rec.*, 2022, **22**, e202100327.
20 D. H. Dai, J. Yang, Y. Wang and Y. W. Yang, *Adv. Funct. Mater.*, 2021, **31**, 2006168.
21 C. B. Liu, X. Y. Chen, B. Y. Zong and S. Mao, *J. Mater. Chem. A*, 2019, **7**, 6616–6630.
22 N. Basu, M. Horvat, D. C. Evers, I. Zastenskaya, P. Weihe and J. Tempowski, *Environ. Health Perspect.*, 2018, **126**, 106001.
23 V. Bhardwaj, V. M. Nurchi and S. K. Sahoo, *Pharmaceuticals*, 2021, **14**, 123.
24 S. O. Aderinto, *Chem. Pap.*, 2020, **74**, 3195–3232.
25 G. Q. Chen, Z. Guo, G. M. Zeng and L. Tang, *Analyst*, 2015, **140**, 5400–5443.
26 S. P. Kollur, C. Shivamallu, S. K. Prasad, R. Veerapur, S. S. Patil, C. A. Cull, J. F. Coetzee and R. G. Amachawadi, *Separations*, 2021, **8**, 192.
27 C. C. Chang, C. P. Chen, T. H. Wu, C. H. Yang, C. W. Lin and C. Y. Chen, *Nanomaterials*, 2019, **9**, 861.
28 X. Wang and J. N. Manikoff, *Gen. Chem.*, 2018, **4**, 180003.
29 W. H. Danial, N. A. S. Mohamed and Z. A. Majid, *Carbon Lett.*, 2022, **32**, 57–80.
30 N. Choudhury and P. De, *J. Macromol. Sci., Part A: Pure Appl.Chem.*, 2021, **58**, 835–848.
31 M. Kasha, *J. Chem. Phys.*, 1952, **20**, 71–74.
32 Z. W. Lu, J. Li, K. Ruan, M. M. Sun, S. X. Zhang, T. Liu, J. J. Yin, X. X. Wang, H. P. Chen, Y. Y. Wang, P. Zou, Q. M. Huang, J. S. Ye and H. B. Rao, *Chem. Eng. J.*, 2022, **435**, 134979.
33 N. Wu, H. Guo, M. Y. Wang, L. P. Peng, Y. Chen, B. Q. Liu, Z. L. Pan, Y. S. Liu and W. Yang, *Spectrochim. Acta, Part A*, 2022, **270**, 120858.
34 Z. Mermer, O. Yavuz, S. K. Atasen, Y. Alcay and I. Yilmaz, *J. Hazard. Mater.*, 2021, **410**, 124597.
35 H. H. Li, X. Q. Huang, M. Mehedi Hassan, M. Zuo, X. Y. Wu, Y. P. Chen and Q. S. Chen, *Microchem. J.*, 2020, **154**, 104563.
36 L. Zhou, Y. H. Lin, Z. Z. Huang, J. S. Ren and X. G. Qu, *Chem. Commun.*, 2012, **48**, 1147–1149.
37 D. Aydın, *European Journal of Science and Technology*, 2019, **17**, 483–490.
38 X. Y. Yan, S. Rahman, M. Rostami, Z. A. Tabasi, F. Khan, A. Alodhayb and Y. Zhang, *ACS Omega*, 2021, **6**, 23504–23514.
39 H. F. Wu and C. L. Tong, *J. Agric. Food Chem.*, 2019, **67**, 2794–2800.
40 W. B. Lu, X. Y. Qin, S. Liu, G. H. Chang, Y. W. Zhang, Y. L. Luo, A. M. Asiri, A. O. Al-Youbi and X. P. Sun, *Anal. Chem.*, 2012, **84**, 5351–5357.
41 J. J. Zeng, L. H. Liao, X. Lin, G. Y. Liu, X. G. Luo, M. Luo and F. S. Wu, *Int. J. Mol. Sci.*, 2022, **23**, 9213.

42 Y. F. Long, D. L. Jiang, X. Zhu, J. X. Wang and F. M. Zhou, *Anal. Chem.*, 2009, **81**, 2652–2657.
43 E. M. Nolan and S. J. Lippard, *Chem. Rev.*, 2008, **108**, 3443–3480.
44 J. R. Lakowicz, *Principles of Fluorescence Spectroscopy*, Springer New York NY, 2006.
45 H. Masuhara, H. Shioyama, T. Saito, K. Hamada, S. Yasoshima and N. Mataga, *J. Phys. Chem.*, 1984, **88**, 5868–5873.
46 N. Saleh, *Luminescence*, 2009, **24**, 30–34.
47 S. Y. Ding, M. Dong, Y. W. Wang, Y. T. Chen, H. Z. Wang, C. Y. Su and W. Wang, *J. Am. Chem. Soc.*, 2016, **138**, 3031–3037.
48 X. J. Zhu, S. T. Fu, W. K. Wong, J. P. Guo and W. Y. Wong, *Angew. Chem., Int. Ed.*, 2006, **45**, 3150–3154.
49 A. M. Costero, R. Andreu, E. Monrabal, R. Martínez-Máñez, F. Sancenón and J. Soto, *J. Chem. Soc., Dalton Trans.*, 2002, 1769–1775.
50 A. Manna, A. K. Maharana, G. Rambabu, S. Nayak, S. Basu and S. Das, *ACS Appl. Polym. Mater.*, 2021, **3**, 5527–5535.
51 Q. R. Tan, X. Y. Li, L. M. Wang, J. Zhao, Q. Y. Yang, P. Sun, Y. Deng and G. Q. Shen, *Front. Chem.*, 2022, **10**, DOI: 10.3389/fchem.2022.1005231.
52 K. Patir and S. K. Gogoi, *ACS Sustain. Chem. Eng.*, 2018, **6**, 1732–1743.
53 J. Yu, N. Song, Y. K. Zhang, S. X. Zhong, A. J. Wang and J. R. Chen, *Sens. Actuators, B*, 2015, **214**, 29–35.
54 F. Noun, E. A. Jury and R. Naccache, *Sensors*, 2021, **21**, 1391.
55 S. W. Wu, Y. Z. Yin, C. Y. Sun and W. J. Song, *ChemistrySelect*, 2022, **7**, e202202540.
56 L. N. Zhang, Y. R. Xu, J. Xu, H. J. Zhang, T. Q. Zhao and L. Jia, *J. Hazard. Mater.*, 2022, **430**, 128478.
57 Y. Qiao, J. R. Guo, D. Li, H. J. Li, X. X. Xue, W. Jiang, G. B. Che and W. S. Guan, *J. Solid State Chem.*, 2020, **290**, 121610.
58 M. J. Ren, H. Wang, Y. Y. Liu, Q. Ma, W. J. Jia, M. Z. Liu, H. J. Wang and Y. C. Lu, *Anal. Lett.*, 2020, **53**, 2700–2714.
59 B. Yan, *Acc. Chem. Res.*, 2017, **50**, 2789–2798.
60 S. Ghosh, F. Steinke, A. Rana and S. Biswas, *Inorg. Chem. Front.*, 2022, **9**, 859–869.
61 R. V. Rathod, S. Bera, P. Maity and D. Mondal, *ACS Omega*, 2020, **5**, 4982–4990.
62 S. Pattnayak, U. Sahoo, S. Choudhury and G. Hota, *Colloids Surf., A*, 2022, **648**, 129377.
63 M. C. Nunes, F. Dos Santos Carlos, O. Fuganti, L. A. Da Silva, H. T. Ribas, S. M. B. Winnischofer and F. S. Nunes, *J. Fluoresc.*, 2020, **30**, 235–247.
64 Z. M. Sahin, D. Alimli, M. M. Tonta, M. E. Kose and F. Yilmaz, *Sens. Actuators, B*, 2017, **242**, 362–368.
65 J. R. Zhang, W. T. Huang, A. L. Zeng, H. Q. Luo and N. B. Li, *Biosens. Bioelectron.*, 2015, **64**, 597–604.
66 V. Bhalla, R. Tejpal, M. Kumar, R. K. Puri and R. K. Mahajan, *Tetrahedron Lett.*, 2009, **50**, 2649–2652.
67 H. L. Tan, B. X. Liu and Y. Chen, *ACS Nano*, 2012, **6**, 10505–10511.
68 E. M. Nolan and S. J. Lippard, *J. Am. Chem. Soc.*, 2003, **125**, 14270–14271.
69 P. Srivastava, S. S. Razi, R. Ali, R. C. Gupta, S. S. Yadav, G. Narayan and A. Misra, *Anal. Chem.*, 2014, **86**, 8693–8699.
70 B. Mohan, Z. Y. Tao, S. Kumar, T. T. Xing, S. X. Ma, W. B. Huang, X. P. Yang, H. Z. You and P. Ren, *Cryst. Growth Des.*, 2022, **22**, 5407–5415.
71 Y. J. Tong, L. D. Yu, N. Li, Q. Fu, K. Xu, J. J. Wei, Y. X. Ye, J. Q. Xu, F. Zhu, J. Pawliszyn and G. F. Ouyang, *Anal. Chim. Acta*, 2021, **1183**, 338967.
72 J. Yang, Z. Wang, Y. S. Li, Q. X. Zhuang, W. R. Zhao and J. L. Gu, *RSC Adv.*, 2016, **6**, 69807–69814.
73 Y. Hou, Y. N. Zhou, S. N. Lu, X. Zhang, H. B. Tai, Y. Y. Zhu, Z. G. Sun, D. P. Dong, C. Q. Jiao and J. R. Li, *Microchem. J.*, 2020, **159**, 105385.
74 S. Erdemir, M. Oguz and S. Malkondu, *Anal. Chim. Acta*, 2022, **1192**, 339353.
75 Y. C. Sun, L. Z. Wang, J. H. Zhou, D. W. Qin and H. D. Duan, *Appl. Organomet. Chem.*, 2020, **34**, e5945.
76 H. Agarwalla, P. S. Mahajan, D. Sahu, N. Taye, B. Ganguly, S. B. Mhaske, S. Chattopadhyay and A. Das, *Inorg. Chem.*, 2016, **55**, 12052–12060.
77 S. Goswami, S. Das and K. Aich, *Tetrahedron Lett.*, 2013, **54**, 4620–4623.
78 E. Ermakova, J. Michalak, M. Meyer, V. Arslanov, A. Tsivadze, R. Guilard and A. Bessmertnykh-Lemeune, *Org. Lett.*, 2013, **15**, 662–665.
79 J. Khan, M. Sadia, S. W. A. Shah, M. Zahoor, K. F. Alsharif and F. A. Al-Joufi, *Arab. J. Chem.*, 2022, **15**, 103710.
80 S. M. Cheung and W. H. Chan, *Tetrahedron*, 2006, **62**, 8379–8383.
81 J. B. Wang, X. H. Qian and J. N. Cui, *J. Org. Chem.*, 2006, **71**, 4308–4311.
82 P. Wei, L. Xiao, Y. T. Gou, F. He, P. Wang and X. P. Yang, *Spectrochim. Acta, Part A*, 2023, **285**, 121836.
83 X. Y. Meng, J. B. Wang, X. Li, Q. Sun, Q. D. Tu, X. H. Liu, H. F. He and F. Zhao, *Microchem. J.*, 2021, **169**, 106551.
84 Y. C. Chen, J. W. Lam, R. T. Kwok, B. Liu and B. Z. Tang, *Mater. Horiz.*, 2019, **6**, 428–433.
85 J. Mei, N. L. Leung, R. T. Kwok, J. W. Lam and B. Z. Tang, *Chem. Rev.*, 2015, **115**, 11718–11940.
86 Y. N. Hong, J. W. Lam and B. Z. Tang, *Chem. Soc. Rev.*, 2011, **40**, 5361–5388.
87 Y. N. Hong, J. W. Lam and B. Z. Tang, *Chem. Commun.*, 2009, 4332–4353.
88 J. D. Luo, Z. L. Xie, J. W. Y. Lam, L. Cheng, H. Y. Chen, C. F. Qiu, H. S. Kwok, X. W. Zhan, Y. Q. Liu, D. B. Zhu and B. Z. Tang, *Chem. Commun.*, 2001, 1740–1741.
89 K. Wang, J. J. Li, S. M. Ji, L. J. Li, Z. P. Qiu, C. Q. Pan, J. Y. Zhang and Y. P. Huo, *New J. Chem.*, 2018, **42**, 13836–13846.
90 J. Ma, Y. L. Zeng, L. L. Yan, B. K. Chen, M. Y. Sun, Z. H. Liu and S. P. Zhang, *Phosphorus, Sulfur Silicon Relat. Elem.*, 2018, **193**, 582–586.
91 W. Y. Fang, G. B. Zhang, J. Chen, L. Kong, L. M. Yang, H. Bi and J. X. Yang, *Sens. Actuators, B*, 2016, **229**, 338–346.
92 A. P. Gao, Q. Q. Han, Q. Q. Wang, R. Wan, H. J. Wu and X. H. Cao, *Gels*, 2022, **8**, 464.

93 H. Yu, K. Ryu, J. Park, S. Subedi and K. H. Lee, *Dyes Pigm.*, 2022, **204**, 110461.
94 T. B. Wei, Q. Zhao, Z. H. Li, X. Y. Dai, Y. B. Niu, H. Yao, Y. M. Zhang, W. J. Qu and Q. Lin, *Dyes Pigm.*, 2021, **192**, 109436.
95 J. Ma, Y. Xiao, C. H. Zhang, M. M. Zhang, Q. Y. Wang, W. G. Zheng and S. P. Zhang, *Mater. Sci. Eng., B*, 2020, **259**, 114582.
96 D. L. Hu, S. J. Liao, X. Chen, J. C. Du, K. Dawood, S. Chauhan, C. Gao and W. Li, *Bull. Korean Chem. Soc.*, 2020, **41**, 686–690.
97 S. J. Jiang, S. B. Chen, Z. C. Wang, H. Y. Guo and F. F. Yang, *Sens. Actuators, B*, 2020, **308**, 127734.
98 X. Q. Ma, Y. Wang, T. B. Wei, L. H. Qi, X. M. Jiang, J. D. Ding, W. B. Zhu, H. Yao, Y. M. Zhang and Q. Lin, *Dyes Pigm.*, 2019, **164**, 279–286.
99 A. L. Tang, Y. Yin, Z. Chen, C. B. Fan, G. Liu and S. Z. Pu, *Tetrahedron*, 2019, **75**, 130489.
100 J. B. Qiu, S. J. Jiang, B. N. Lin, H. Y. Guo and F. F. Yang, *Dyes Pigm.*, 2019, **170**, 107590.
101 Y. Q. Wu, X. Y. Wen and Z. F. Fan, *Spectrochim. Acta, Part A*, 2019, **223**, 117315.
102 Y. R. Li, Y. Liu, H. T. Zhou, W. Chen, J. Mei and J. H. Su, *Chem.–Eur. J.*, 2017, **23**, 9280–9287.
103 Y. R. Li, H. T. Zhou, W. Chen, G. C. Sun, L. Sun and J. H. Su, *Tetrahedron*, 2016, **72**, 5620–5625.
104 L. Liu, G. X. Zhang, J. F. Xiang, D. Q. Zhang and D. B. Zhu, *Org. Lett.*, 2008, **10**, 4581–4584.
105 H. Zhang, Y. Qu, Y. T. Gao, J. L. Hua, J. Li and B. Li, *Tetrahedron Lett.*, 2013, **54**, 909–912.
106 J. T. Yang, B. S. Yang, G. M. Wen and B. Liu, *Sens. Actuators, B*, 2019, **296**, 126670.
107 Q. S. Liu, Z. H. Yang, Z. L. Wang, Y. Sun, L. L. Chen, L. Sun, X. B. Sun and W. Gu, *J. Photochem. Photobiol., A*, 2022, **423**, 113597.
108 K. S. Jagadhane, S. R. Bhosale, D. B. Gunjal, O. S. Nille, G. B. Kolekar, S. S. Kolekar, T. D. Dongale and P. V. Anbhule, *ACS Omega*, 2022, **7**, 34888–34900.
109 Z. H. Zhang, Y. M. Zhang, X. T. Kan, Q. Y. Yang, Y. J. Li, T. B. Wei, H. Yao and Q. Lin, *Dyes Pigm.*, 2021, **191**, 109389.
110 G. Wei, Y. L. Jiang and F. Wang, *Tetrahedron Lett.*, 2018, **59**, 1476–1479.
111 A. Gautam, P. Komal, P. Gautam, A. Sharma, N. Kumar and J. P. Jung, *Metals*, 2021, **11**, 329.
112 A. L. Feng, Q. Y. Jiang, G. G. Song, Z. Xu and X. Q. Liu, *Chin. J. Anal. Chem.*, 2022, **50**, 100118.
113 R. Liu, S. S. Duan, L. J. Bao, Z. Y. Wu, J. Zhou and R. Q. Yu, *Anal. Chim. Acta*, 2020, **1114**, 50–57.
114 J. J. Li, Q. Dan, J. Zhao, G. J. Weng, J. Zhu and J. W. Zhao, *Methods Appl. Fluoresc.*, 2019, **7**, 45001.
115 H. H. Deng, X. Y. Fang, K. Y. Huang, S. B. He, H. P. Peng, X. H. Xia and W. Chen, *Anal. Chim. Acta*, 2019, **1088**, 116–122.
116 L. Y. Yu, L. Y. Zhang, G. J. Ren, S. Li, B. Y. Zhu, F. Chai, F. Y. Qu, C. G. Wang and Z. M. Su, *Sens. Actuators, B*, 2018, **262**, 678–686.
117 Y. Y. Zhang, H. Jiang and X. M. Wang, *Anal. Chim. Acta*, 2015, **870**, 1–7.
118 D. Y. Cao, J. Fan, J. R. Qiu, Y. F. Tu and J. L. Yan, *Biosens. Bioelectron.*, 2013, **42**, 47–50.
119 F. Li, J. Wang, Y. M. Lai, C. Wu, S. Q. Sun, Y. H. He and H. Ma, *Biosens. Bioelectron.*, 2013, **39**, 82–87.
120 M. R. Knecht and M. Sethi, *Anal. Bioanal. Chem.*, 2009, **394**, 33–46.
121 J. Lee, M. S. Han and C. A. Mirkin, *Angew. Chem., Int. Ed.*, 2007, **46**, 4093–4096.
122 J. P. Xie, Y. G. Zheng and J. Y. Ying, *Chem. Commun.*, 2010, **46**, 961–963.
123 D. Sahu, P. Mohapatra and S. K. Swain, *J. Photochem. Photobiol., A*, 2020, **386**, 112098.
124 X. J. Nan, Y. C. Huyan, H. J. Li, S. G. Sun and Y. Q. Xu, *Coord. Chem. Rev.*, 2021, **426**, 213580.
125 M. Zeinali and A. Torrents, *Environ. Sci. Technol.*, 1998, **32**, 2338–2342.
126 Y. F. Han, C. Y. Yang, K. Wu, Y. Chen, B. C. Zhou and M. Xia, *RSC Adv.*, 2015, **5**, 16723–16726.
127 M. Santra, B. Roy and K. H. Ahn, *Org. Lett.*, 2011, **13**, 3422–3425.
128 X. Shang, N. X. Wang, R. Cerny, W. Niu and J. T. Guo, *ACS Sens.*, 2017, **2**, 961–966.
129 J. Tang, H. Wu, S. Yin and Y. F. Han, *Tetrahedron Lett.*, 2019, **60**, 541–546.
130 H. J. Chun, S. Kim, Y. D. Han, D. W. Kim, K. R. Kim, H. S. Kim, J. H. Kim and H. C. Yoon, *Biosens. Bioelectron.*, 2018, **104**, 138–144.
131 H. Zhang, Z. X. Lei, X. Fu, X. C. Deng, Q. Wang and D. Y. Gu, *Sens. Actuators, B*, 2017, **246**, 896–903.
132 Z. H. Li, H. J. Sun, X. Y. Ma, R. F. Su, R. Sun, C. Y. Yang and C. Y. Sun, *Anal. Chim. Acta*, 2020, **1099**, 136–144.
133 N. Xia, F. Feng, C. Liu, R. Q. Li, W. W. Xiang, H. X. Shi and L. Gao, *Talanta*, 2019, **192**, 500–507.
134 X. X. Lv, W. C. Wu, C. G. Niu, D. W. Huang, X. Y. Wang and X. G. Zhang, *Talanta*, 2016, **151**, 62–67.
135 Y. Li, N. Liu, H. Liu, Y. Wang, Y. W. Hao, X. H. Ma, X. L. Li, Y. P. Huo, J. H. Lu, S. G. Tang, C. Q. Wang, Y. H. Zhang and Z. X. Gao, *Sci. Rep.*, 2017, **7**, 45974.
136 J. X. Yuan, A. Shen, X. H. Hao, M. Du, X. Y. Du, S. F. Ma, M. W. Li, L. F. Zhang and Y. X. Yang, *New J. Chem.*, 2022, **46**, 5966–5974.
137 Z. M. Zhong, D. D. Zhang, D. M. Li, G. X. Zheng and Z. Z. Tian, *Tetrahedron*, 2016, **72**, 8050–8054.
138 Y. Shinohara, K. Tsukamoto and H. Maeda, *J. Photochem. Photobiol., A*, 2019, **371**, 407–413.
139 Y. Y. Gao, N. Yi, Z. Z. Ou, Z. Y. Li, T. T. Ma, H. D. Jia, W. L. Xing, G. Q. Yang and Y. Li, *Sens. Actuators, B*, 2018, **267**, 136–144.
140 Z. L. Wang, Y. Zhang, J. Yin, Y. Q. Yang, H. Luo, J. Song, X. Xu and S. F. Wang, *ACS Sustain. Chem. Eng.*, 2020, **8**, 12348–12359.
141 V. Dujols, F. Ford and A. W. Czarnik, *J. Am. Chem. Soc.*, 1997, **119**, 7386–7387.
142 Y. J. Wang, X. J. Wang, W. Y. Ma, R. H. Lu, W. F. Zhou and H. X. Gao, *Chemosensors*, 2022, **10**, 399.

143 H. N. Kim, M. H. Lee, H. J. Kim, J. S. Kim and J. Yoon, *Chem. Soc. Rev.*, 2008, **37**, 1465–1472.
144 S. Y. Ma, Y. Q. Wang, M. Y. She, S. Wang, Z. Yang, P. Liu, S. Y. Zhang and J. L. Li, *Rev. Anal. Chem.*, 2017, **36**, 20160024.
145 Y. Yang, K. Yook and J. Tae, *J. Am. Chem. Soc.*, 2005, **127**, 16760–16761.
146 P. Ozmen, Z. Demir and B. Karagoz, *Eur. Polym. J.*, 2022, **162**, 110922.
147 Z. G. Gao, S. Y. Qiu, M. C. Yan, H. B. Liu, S. H. Lu, H. H. Lian, P. Zhang, J. Zhu and M. J. Jin, *J. Mol. Struct.*, 2022, **1254**, 132312.
148 T. Li, W. Zhou, Q. S. Song and W. C. Fang, *J. Photochem. Photobiol., A*, 2015, **302**, 51–58.
149 A. Petdum, N. Faichu, J. Sirirak, P. Khammultri, V. Promarak, W. Panchan, T. Sooksimuang, A. Charoenpanich and N. Wanichacheva, *J. Photochem. Photobiol., A*, 2020, **394**, 112473.
150 B. D. Vanjare, P. G. Mahajan, H. Ryoo, N. C. Dige, N. G. Choi, Y. Han, S. J. Kim, C. H. Kim and K. H. Lee, *Sens. Actuators, B*, 2021, **330**, 129308.
151 B. Yan, *Inorg. Chem. Front.*, 2021, **8**, 201–233.
152 S. E. Bodman and S. J. Butler, *Chem. Sci.*, 2021, **12**, 2716–2734.
153 S. N. Zhao, G. B. Wang, D. Poelman and P. V. D. Voort, *Materials*, 2018, **11**, 572.
154 F. Ahmed, S. Iqbal and H. Xiong, *Environ. Sci.: Nano*, 2022, **9**, 2624–2637.
155 C. Correia, J. Martinho and E. Maçôas, *Nanomaterials*, 2022, **12**, 385.
156 W. L. Liu, A. M. Kaczmarek, P. Van Der Voort and R. Van Deun, *Dalton Trans.*, 2022, **51**, 11467–11475.
157 R. Singhaal, L. Tashi, S. Devi and H. N. Sheikh, *New J. Chem.*, 2022, **46**, 6528–6538.
158 H. Guo, X. Q. Wang, N. Wu, M. N. Xu, M. Y. Wang, L. W. Zhang and W. Yang, *Anal. Chim. Acta*, 2021, **1141**, 13–20.
159 R. F. Li, Y. W. Zhang, X. F. Liu, X. H. Chang and X. Feng, *Inorg. Chim. Acta*, 2020, **502**, 119370.
160 P. Y. Lv, Y. Cao, Z. Liu, R. Wang, B. X. Ye and G. P. Li, *Anal. Methods*, 2020, **12**, 91–96.
161 X. X. Zhang, W. J. Zhang, C. L. Li, X. H. Qin and C. Y. Zhu, *Inorg. Chem.*, 2019, **58**, 3910–3915.
162 H. W. Chien, C. H. Wu, C. H. Yang and T. L. Wang, *J. Alloys Compd.*, 2019, **806**, 272–282.
163 D. Y. Liu, K. Z. Tang, W. S. Liu, C. Y. Su, X. H. Yan, M. Y. Tan and Y. Tang, *Dalton Trans.*, 2010, **39**, 9763–9765.
164 N. W. H. Guo, L. P. Peng, Y. Chen, Y. S. Liu, C. L. Li, H. Zhang and W. Yang, *Talanta*, 2022, **250**, 123710.
165 S. J. Wang, Q. Li, G. L. Xiu, L. X. You, F. Ding, R. Van Deun, I. Dragutan, V. Dragutan and Y. G. Sun, *Dalton Trans.*, 2021, **50**, 15612–15619.
166 X. Y. Xu and B. Yan, *Adv. Funct. Mater.*, 2017, **27**, 1700247.
167 X. Y. Xu and B. Yan, *J. Mater. Chem. C*, 2016, **4**, 1543–1549.
168 T. F. Xia, T. Song, G. G. Zhang, Y. J. Cui, Y. Yang, Z. Y. Wang and G. D. Qian, *Chem.–Eur. J.*, 2016, **22**, 18429–18434.
169 H. Wang, X. L. Wang, M. S. Liang, G. Chen, R. M. Kong, L. Xia and F. L. Qu, *Anal. Chem.*, 2020, **92**, 3366–3372.